Non-destructive tests in roads and airfields

A study of the Falling Weight Deflectometer

Edgar Alexandre Chong Cardoso

Thesis to obtain the Master of Science Degree in

Civil Engineering

Supervisor: Prof. José Manuel Coelho das Neves

Examination Committee

Chairperson: Prof. João Torres de Quinhones Levy

Supervisor: Prof. José Manuel Coelho das Neves

Members of the Committee: Prof. Luís Guilherme de Picado Santos

November 2017

Acknowledgement

The present dissertation was developed with close guidance and supervision of Professor Doctor José Neves whom I wish to extend my immense gratitude towards his dedication in the completion of this project. Without his belief and enthusiasm this work would not have been possible. It is my great pleasure to thank those who made this thesis possible, the institutions involved in the experimental research included in this work.: Instituto Superior Técnico (Professor Doctor Luís Picado Santos and César Abreu), Laboratório Nacional de Engenharia Civil (Vitor Antunes, Vânia Marecos), Força Aérea Portuguesa – Laboratório Solos e Pavimentos (Lieutenant Henrique Rodrigues and the officers involved). The proficiency test was organized under coordination of RELACRE, with Cláudia Silva and Ana Maria Duarte, whom kindly released all data necessary in developing this project.

To my Parents that endured so much and did not stop motivating me through hardship for so long.

To my grandfather Ming Lam whom I miss dearly and wished he could witness my achievements.

To my cousin Noel for the long hours of motivation talk and guidance.

To all my friends that provided the utmost support and belief at all times. My special thanks to Paulo Chainho and Ana Rita Martins, who contributed to the completion of the project.

To the medical staff that have given me a second chance to live fully.

Lastly, I would like to send my best regards to all those who were directly or indirectly involved in any respect during the completion of this dissertation.

Resumo

O património rodoviário é um ativo de elevada importância no desenvolvimento das sociedades modernas e a sua qualidade geral desempenha um papel fundamental na segurança, economia, competitividade e sustentabilidade da circulação de pessoas e bens. A degradação dessa qualidade ao longo do tempo deve ser avaliada de forma a que as ações de conservação e reabilitação possam ser adequadamente planeadas para assegurar os padrões mínimos de qualidade especificados. No âmbito do estado dos pavimentos, são vários os indicadores estabelecidos na avaliação da qualidade. Em termos da avaliação estrutural, o defletómetro de impacto – Falling Weight Deflectometer (FWD) – é o ensaio não destrutivo mais utilizado na avaliação da capacidade de carga de pavimentos rodoviários e aeroportuários. Os resultados deste ensaio são da maior importância em vários contextos, como por exemplo na auscultação estrutural dos pavimentos existentes em obras de reabilitação de infraestruturas rodoviárias ou aeroportuárias.

A presente dissertação tem como objetivos principais a avaliação da precisão e da incerteza das deflexões medidas no ensaio com o FWD e a análise da sua influência na qualidade de interpretação desses mesmos ensaios, ou seja, das características de deformabilidade dos pavimentos existentes obtidas por retroanálise, com vista à avaliação da sua qualidade estrutural e apoio ao projeto de reabilitação.

A metodologia adotada baseou-se na realização de um ensaio de aptidão segundo a norma ISO/IEC 17043 com a participação de três equipamentos de fabricantes diferentes e pertencentes a entidades nacionais. Os resultados obtidos foram analisados quanto à repetibilidade e reprodutibilidade e, posteriormente, procedeu-se à quantificação da incerteza. Atendendo aos resultados obtidos nesta análise, procedeu-se a um estudo de sensibilidade da influência da incerteza das deflexões medidas nos módulos de deformabilidade das camadas do pavimento e fundação, obtidos da interpretação dos resultados dos ensaios (retroanálise) para o caso de pavimentos flexíveis.

Em geral, os resultados confirmaram uma boa repetibilidade das deflexões, contrastando com níveis por vezes muito baixos de reprodutibilidade. Por consequência, a incerteza revelou-se grande. Constatou-se ainda que a precisão e a incerteza dependeram do tipo de pavimento e da magnitude das deflexões. A incerteza foi maior em pavimentos flexíveis e para deflexões também maiores. Em relação à análise de sensibilidade da influência da incerteza na interpretação dos resultados do FWD, verificou-se que a sensibilidade à incerteza é maior em pavimentos mais flexíveis, nomeadamente em relação à análise da deformabilidade dos materiais da fundação.

Palavras-chave: *defletometro de impacto, pavimentos, repetibilidade, reprodutibilidade, incerteza, retroanálise*

Abstract

Road infrastructure is a high value asset in the development of modern society where its perceived quality translates into a fundamental role in security, economy, competitivity and sustainability of the free flow of people and goods. The gradual degradation of that quality through time should be evaluated in such a manner that maintenance and rehabilitation efforts can be timely planned and carried out to maintain its specified minimum quality requirements. In pavement condition assessment, there are several parameters that gauge pavement quality. The Falling Weight Deflectometer (FWD), is the main non-destructive testing equipment used to assess the bearing capacity of road and airfield pavements. This test's results are very relevant in several contexts, for example, a survey for bearing capacity in existing road or airfield pavements requiring rehabilitation intervention.

The present dissertation's objective is to assess the precision and uncertainty performance in measuring deflection and to analyze its influence in the quality of results from the testing campaign, therefore assessing the structural capacity of existing pavements (backanalysis), in view to evaluate the structural quality and support a rehabilitation project.

The adopted methodology consisted in a proficiency test scheme (PTS) field test compliant with ISO/IEC 17043 featuring a fleet of three FWD from different manufactures and owned by portuguese operators. The obtained deflection data was firstly processed for repeatability and reproducibility, and afterwards analyzed for uncertainty quantification. Lastly, the resulting data was used for a sensitivity analysis featuring the uncertainty of the measured deflection influence on the mechanical properties (elastic moduli) estimated from the field survey (backanalysis) on flexible pavements.

The experimental research results confirmed a satisfactory repeatability of deflection measurements. In contrast, the reproducibility is difficult to achieve in most cases. Consequently, the uncertainty levels revealed to be high. Uncertainty and precision revealed to be dependent of pavement type and deflection magnitude. Uncertainty presented high values for flexible pavement and for high deflections. Regarding to the sensitivity analysis on the uncertainty's influence on the FWD results interpretation, it was concluded that the flexible pavements presented higher sensibility to uncertainty mainly when gauging for stiffness on the foundation layers.

Keywords: *falling weight deflectometer, pavements, repeatability, reproducibility, uncertainty, backcalculation*

Table of contents

List of figures

List of tables

Abbreviations

AASHO	American Association of States Highways Officials
AASHTO	American Association of State Highway and Transportation Officials
ASTM	American Society for Testing and Materials
BC	Backcalculation
EuroFWD	European Falling Weight Deflectometer User Group
FWD	Falling Weight Deflectometer
FWDUG	Falling Weight Deflectometer User Group
GPR	Ground Penetrating Radar
HWD	Heavy Weight Deflectometer
IST	Instituto Superior Técnico
LDVT	Linear Differential Vertical Transducers
LNEC	Laboratório Nacional de Engenharia Civil
LSP	Laboratório de Solos e Pavimentos – Força Aérea Portuguesa
LTPP	Long-Term Pavement Performance
LWD	Light Weight Deflectometer
M&R	Maintenance and rehabilitation
MACOPAV	Manual de Concepção de Pavimentos para a Rede Rodoviária Nacional
MEPDG	Mechanistic-Empirical Pavement Design Guide
NCAT	National Center for Asphalt Institute
NCHRP	National Cooperative Highway Research Program
NDT	Non-Destructive Test
PMS	Pavement Management System
PTS	Proficiency Test Scheme
RDT	Road Deflection Tester
RELACRE	Associação de Laboratórios Acreditados de Portugal
RMSE	Root Mean Square Error
SF	Smoothing Filter
TSD	Traffic Speed Deflectometer

1 Introduction

1.1 Background and aim

Looking at the European Union statistic data, the Trans-European networks in transport (TEN-T) plays a vital role to promote people and goods circulations between member states (Eurostat, 2014). By promoting business and easy people circulation, transportation strategies are an effective way to tackle inclusion of state members and its citizens. Eurostat data referring to modal split of transportation in EU (Eurostat, 2017) shows that road transport is still by far the most common, representing about 75% of total tonne-kilometers of freight transported. Data forecasts expect a continuing rise of freight transport by road in the foreseeable future. Consequently, new and existing infrastructure assets can benefit from planned maintenance to prolong its life span and reduce the involved financial costs. In a report commended by the European Commission (Steer Davies Gleave, 2009), EU countries invested in total €859 billion in its transport infrastructure sector between 2000 and 2006. A significant portion of the budget was used towards road maintenance to keep existing infrastructures at an acceptable level of service. This sector has proven its significance given the large sum invested thus incentivizing pavement engineering to continually improve (COST, 1997).

Maintenance and rehabilitation (M&R) requires both minimizing administration and user costs while still maintaining infrastructures at high level of service (Meneses & Ferreira, 2012). To manage pavements at network level, administration rely on pavement management systems (PMS) which aggregate road condition data by road sections. This information is in turn analyzed to clearly prioritize interventions to the most critical road sections (Fwa, et al, 2000). Road and airfield administrations are the main clients for the services provided by pavement condition assessment companies. These survey proceedings are regulated by international standards (ASTM, 2008, 2009) using equipment capable of measuring and recording pavement parameters to assessment its condition. One of the most used equipment today is the Falling Weight Deflectometer (FWD), a stationary impulse load deflectometer which will be studied in depth in the following sections of present dissertation.

Although equipment manufacturers guarantee high reliability and repeatability levels through periodic calibration, generally, equivalent models from different manufacturers are less likely to reproduce each other's measurements. Several authors research (Garg, 2002; Murphy, 1998; Rocha et al, 2004) mention the repeatability and reproducibility issues associated with the FWD which should be taken in consideration and carefully assessed in practice. To empower administration decision makers with informed decisions while executing pavement surveys, it is necessary to experimentally analyze the actual reliability level of existing FWD fleets in current available service providers and thus clearly quantifying existing differences.

This dissertation aims to investigate the precision performance of a FWD fleet under a controlled environment, and mainly to quantify the level of uncertainty in deflection measurements which ultimately influence the quality of the backcalculation process. It is crucial for the administration to have a good understanding of the uncertainty involved in this process which may lead to rehabilitation project designs that may prove to be ineffective and financially inefficient.

1.2 Objectives

The present dissertation objectives are:

i. Assess FWD uncertainty and precision performance in measuring deflection with actual collection of test data;

ii. Assess uncertainty's influence on the quality of backcalculated elastic moduli by perform a sensitivity analysis.

1.3 Methodology

The dissertation presents a thorough literature review about non-destructive pavement testing and the available analytic methods. The first part of the dissertation focuses on reviewing relevant journals and papers currently available on pavement engineering on both network level and project level. This approach provides the necessary framework for the subjects studied in this work. After a brief introduction to NDT, the FWD is fully described, with special emphasis to the components that are reported to be the main sources of FWD uncertainty.

A field test is organized to gather several FWD equipment from various operators. To provide the necessary experimental data, a proficiency test scheme compliant with norm ISO/IEC 17043 (ISO, 2010) was devised to measure pavement deflections in a predetermined test site. From the experimental data, repeatability and reproducibility analysis compliant with ISO 5725-2 is performed. The results are used to frame the experiment for an uncertainty assessment which studies intervals of maximum and minimum values of deflections produced for any given measurement.

Finally, through a set of previously chosen standardized theoretical pavements models (JAE, 1995), a linear elastic layer model computer software BISAR (Shell, 1995) was used to perform backcalculations to assess the respective pavement stiffness. A sensitivity analysis on the resulting elastic moduli is performed to study the influence of the FWD uncertainty on the quality of backcalculation. As a final case study, Test site 1 is backcalculated and the results analyzed.

1.4 Dissertation structure

This dissertation is subdivided in a total of five chapters:

- Chapter 1, is the introductory section where the chosen subject is framed. The dissertation's aim, objectives, adopted methodology and the dissertation structure is announced as the guideline for this project.
- Chapter 2 follows with a thorough literature review on various key subjects such a brief introduction on non-destructive road tests, and specifically, the bearing capacity test equipment FWD. An in-depth FWD study is performed mainly focusing in detail its functional components that are identified as sources of errors, uncertainty and precision issues. A brief reference to concepts of backcalculation methods is also included.
- Chapter 3 presents the experimental research preparation and findings, in which a joint proficiency test is developed with a fleet of three FWD. A test protocol is devised and the FWD equipment are introduced. The measured test results are discussed and expressed through deflection graphs and tables.

- Chapter 4 is centered in performing a thorough data analysis using data from Chapter three. Repeatability and reproducibility analysis is performed resulting in their respective limit values. The deflection measurement uncertainty is also assessed by calculating deflection critical value intervals as function of deflection. The analysis continues with a sensitivity analysis of backcalculated layer moduli to study the impact of FWD uncertainty and its consequence in pavement design.
- In Chapter 5, a summary of the dissertation with final conclusions are presented. Together with future research recommendations in view to promote further development in this field of study.

Finally, the Appendix section is presented in the remaining pages with an extensive collection of tables and plot graphs obtained from the data analysis from Chapter 3 and Chapter 4.

2 Literature review

2.1 Nondestructive pavement tests

2.1.1 Introduction

Since the 1950's, both North America and European countries have been developing techniques to aid field surveys. Most administrations begun to turn their focus to planned repair and maintenance of existing roads rather than continuously build newer structures. A better knowledge in pavement engineering became crucial to develop longer lasting pavements while maintaining high service levels. Pioneering campaigns such as the WASHO (1952-1954) (WASHO, 1954) and AASHO Road Test (1963) (AASHO, 1962) (Figure 2.1) marked the beginning of the development of pavement engineering and with it started the research and development of equipment capable of performing pavement tests and measurements. Non-destructive tests (NDT) became more relevant in modern times as it enabled maintenance without complete service disruption or exposing workers to danger during road works. The first NDT equipment was deflection measuring devices like the Benkelman system and the Lacroix deflectograph. By relating vertical displacement readings to the pavement structural rigidity, it is possible to estimate "in situ" the under layers bearing capacity.

Figure 2.1 - Benkelman Beam in use AASHO Road Test, ca 1962 (Alvin Benkelman Jr.)

Road maintenance management has since changed its paradigm to a business-like asset management approach, in which road administrations manage operations, maintenance and road network development to maintain its value and meet road users satisfaction (Madelin, 2000). The shift towards asset management developed the necessity for a network level approach. Road management can be divided into two different levels of strategy, a "network level" and a "project level". The "network level" manages the road system as a set of roads arranged in different classes defined by their function, traffic, and provides a general overview of the pavements bearing capacity. This level of management focuses mainly on financial and economic issues of maintenance and rehabilitation works. It is also at this level that the main strategy for maintenance prioritization and scheduling is decided as well as the necessary executive budget (Picado-Santos et al, 2006 and COST, 1998). Once network level strategy is defined, "project level" pavement tests can provide further detailed pavement parameters like layer composition, thickness and

stiffness. These pavement tests are more specific to a individual sections of the road network. It mainly deals with the selection of the best methods to test and diagnose issues with the pavement. As focus shifts to maintaining existing infrastructures, it's crucial to keep an up to date database of road network condition. The Pavement Management System (PMS) database includes information of pavement design features, its geometry and subgrade material composition, past maintenance interventions as well as surface distress evidence such as the location of rutting, cracking and reflective cracking (Fontul, 2004).

Currently, the most widely adopted standard equipment for deflection measurement is the Falling Weight Deflectometer (FWD). The FWD generates a vertical impulse by a falling weight and records the induced surface vertical displacement measured with adjacent geophones. Due to its operating characteristic, the FWD is a suitable project level equipment capable of defining the entire deflection basin beneath the surface and, therefore, providing detailed data necessary for multilayered model backanalysis. FWD's can be found in different sizes and capacities. Depending on the maximum load capable to generate, it can be either called the Light Weight Deflectometer or the Heavy Weight Deflectometer. The LWD is hand portable while the HWD is specifically used for aircraft runways and taxi ways. Albeit its versatility, FWD are is still considered too slow to be used in network level surveys.

Road pavements are assets with a limited life span. To design a pavement, it is required to elaborate a model capable to withstand the loads and inner stresses from both the road traffic and the climate. These inputs serve as boundaries from which the mechanistic-empirical design model (MEPDG) should compute a compatible model in a trial basis iterative process.

NDT have been gaining acceptance in both design and maintenance phases. Surface distress analysis systems are currently well developed and there are highly efficient image scanning equipment onboard vehicles capable of operating in normal traffic speeds providing live accurate road analysis. Ground penetrating radar (GPR) and surface laser profilers are also commonly used to assess pavement layer thickness and surface distresses, respectively. However, bearing capacity analysis methods are less developed as they often are based on slow moving equipment and indirect inverse calculation methods. Currently most road agencies rely solely on static or slow-moving wheeled equipment to perform in-situ tests. These slow systems impact the traffic flow and exposes operators to traffic hazards.

2.1.2 Road surface condition

Road surface condition is commonly associated with the local authority's effort for road maintenance. Commuters navigate roads in a daily basis encountering situations of faulty roads poising safety issues and administrations are ultimately held liable in these situations. Since maintenance and rehabilitation intervention is funded by public money, it is important for authorities to consider continuous monitoring and closely track the evolution of road deterioration while strategically manage resources. COST 325 report (COST, 1998) provides a comprehensive essay about current road monitoring equipment and monitoring systems where questionnaires were sent to various participating European countries. The report aggregates different existing practices reported to be in practice. Surface parameters such as poor skid resistance, insufficient macrotexture and wheel track rutting are most important for road safety. Other relevant parameters such as longitudinal unevenness affect ride quality and comfort. Deterioration of these parameters are linked to the increase of traffic loading and the consequent shortening of pavement life span.

Pavement surface distresses such as cracking, rutting and damaged construction joints are directly related to underlying pavement structural problems (Fontul, 2004). The guidelines for identification and severity qualification of such distresses are well documented (Antunes, 1997; ASTM, 1999; AUSTROADS, 2006, 2007a, 2007b, 2008, 2009a, 2009b, 2009c, 2011; Clarke, Harris, Heitzman, & Margiotta, 2003; JAE, 1997; Johnson, 2000; NPMA, 1999) and a correct diagnosis for the underlying issue is essential for an effective rehabilitation procedure.

Since 2009, Portugal have had various campaigns scanning national road network for surface deterioration signs, each cycle taking two full years for complete network coverage. Between 2009 and 2010, it was used a software VIZIROAD to register distress parameters by human visual inspection overlaid with GPS position data. This method had a completion rate of only 80 km per day. In the period of 2011 and 2012, using a newly bought road profiling equipment, the entire network was to be rescanned, producing this time an automatic analysis for parameters such as road surface evenness, surface macrotexture and road geometry parameters such as longitudinal and transversal slope values. With a total of 14 laser sensors, it was also able to scan and calculate rutting depths, record singularities such as the position of bridges, small local urban areas, roundabouts and distance markers. It was also possible to register other types of distresses such as road cracks (Santinho Horta et al, 2011).

2.1.3 Bearing capacity assessment

Although pavement surface condition is readily accessible to road monitoring equipment, assessment of underlying layer condition requires sophisticate methods using a mechanistic approach. Road pavements are mainly constituted by conjoining layers of a determined thickness on top of a subgrade layer. From top to bottom, the surface layer main function is to guarantee a safe and comfortable interface between the structural underlying layers with the road user's vehicle wheels. The structural capacity of the road pavement is provided by stacking several layers of granular material designed to sustain the required traffic load (Branco et al, 2008; Francisco, 2012).

The key physical property for pavement characterization is the static elastic modulus (Oshone et al, 2017). In pavement engineering, this parameter indicates the stiffness of the materials and it is backcalculated from measured vertical displacement known as surface deflection. It is current standard practice that bearing capacity of these multi-layered pavement systems be assessed with nondestructive tests. In contrast with destructive tests, NDT are less disruptive on traffic and require significantly less manpower and time, which in turn decreases the overall cost of the operation. The parameter measured by NDT is generally the pavement deflection (measured in μm) under an applied load. Under normal usage, road pavements are designed with a serviceable period in mind before any rehabilitation intervention is required to assure a prolonged life of the structure. Through periodic monitoring campaigns, measured deflections of the same pavement sections tend to increase over time due to repeated traffic loading. COST action 325 (COST, 1997) lists the existing deflection measurement equipment and groups them in 4 main categories, varying on the level of automation and the load delivery method. Table 2.1 presents this list of different deflection measurement equipment categories and the respective equipment types.

Table 2.1 – Categories of deflection measurement equipment

Category	Equipment
Manual, static or rolling wheel load methods	Load plate Benkelman Beam
Automated, rolling wheel methods	Lacroix deflectograph Curviamètre
Automated, stationary impulse load methods	Falling Weight Deflectometer
Automated, mobile dynamic load methods	Road deflection tester Traffic Speed Deflectometer

A network level survey on pavement structural condition is for many administrations a daunting task, usually associated with high operation cost and possibly unwanted traffic disturbance caused by in-situ workers performing tasks using static or slow-moving equipment. To attend the needs of European road administration, several surveys have been conducted over the years investigating needs and the necessary capabilities for new equipment and methods for retrieving pavement condition data. COST action 325 (COST, 1997) found that the Falling Weight Deflectometer and the Lacroix systems were the most popular deflectograph used by majority of countries. HeRoad (Benbow & Wright, 2012) concluded that European administrations perceive pavement durability as an important issue and traffic speed capable equipment is sought for. FORMAT (*FORMAT*, 2005) reported the existence of two traffic speed deflectographs developed in Sweden and in Denmark. The Swedish Road Deflection Tester (RDT) and the Danish High Speed Deflectograph (HSD) now renamed as Traffic Speed Deflectometer (TSD).

Figure 2.2 – Traffic Speed Deflectometer (ARRB Group Inc. USA)

The TSD technology are based in automatic vertical velocity measurements of deflected pavement surface using Doppler lasers techniques with 3 to 10 vibrometers on board (Andersen et al, 2017). The equipment is installed in the back of a semi-trailer truck and requires only the driver to operate the whole system. The loading is done by the truck's semi-trailer wheel axle at traffic speeds between 40-80 kmph. The measurements are continuous as necessary for network level survey. Like the FWD, these traffic speed deflectometers also need prior knowledge of the material constitution of the layers and its respective thickness. Incorrect estimation of the thickness can cause erratic stiffness calculation results, therefore it is highly recommended to perform auxiliary in-situ tests to gather additional information. In these cases, the Ground Penetrating Radar (GPR) is a valid NDT to assess layer thickness. Together, TSD and GPR provide a viable solution to network level structural condition assessments (Wright et al., 2016). Traffic speed deflectometers together with PMS will surely become a standard practice in the future for road administrations enabling minimum traffic disruption while automatizing the process, although only if this technology proves to be cost effective and effective (Andrén, 2006).

2.2 Falling Weight Deflectometer

2.2.1 Introduction

The FWD is one of the most used deflection measuring equipment preferred by administrations (Flores et al, 2017). It is simple to transport on a trailer and it can be entirely mounted inside a van. The basic concept behind the FWD (Čičković, 2017) is the pavement mechanics behavior that enables the assessment of pavement stiffness when inducing localized vertical displacements (Elastic Multilayer Theory). A pulse load is induced by dropping a suspended mass at a predetermined height, while a system of loading plates and buffers transmit the exerted load to the surface. The pulse of load generated has a characteristic half sine shaped curvature exactly similar to loads that would be generated by a standard truck wheel axles or aircraft wheels (in case of airfield application). As the surface load dissipates in the underneath layers, the FWD captures and records surface vertical displacements in an array of geophones evenly spaced and radially away from the center of the drop. The main characteristic of the FWD when comparing to other deflectographs is its unique ability to calculate the complete deflection basin generated by the load pulse. The geophone array is usually constituted by a series of 9 geophones installed in a straight mount bar that automatically lowers to contact with the surface prior to the weight drop moment. The process completes as the recorded deflection data is processed by a backcalculation software, which with a defined pavement layer model, results in estimated layer stiffness values.

The applied load from the falling mass is variable depending on the test specification, it can range from 40 kN up to 240 kN. For even higher loads there is a heavy version of the FWD, the Heavy Weight Deflectometer (HWD), intended to be used in airfields and is capable of simulating wheel loads up to 320 kN such as the 777 or A340/380.

Figure 2.3 – Falling Weight Deflectometer

Figure 2.4 – Heavy Weight Deflectometer

The FWD was developed in the 1960's, a period where pavement testing where mostly executed with French engineered systems such as the Benkelman Beam and the Lacroix-type deflectometers (Bohn, 1989). The research and development of the FWD was primarily conducted by the Danish Road Laboratory. The main objective with the prototype of the falling weight mechanism was to correctly emulate the load cycle of a vehicle wheel on the pavement surface. A final solution was achieved by adopting a dampening system consisting of a rubber buffer between the falling weight and the loading plate pressing on the road surface. This way, the desired load cycle would be achieved: the falling weight would generate a sine shaped load curve and a load-pulse of 25-30 ms would be reached, similar to the load-of a road vehicle rolling past in normal traffic speeds. The first iterations of the FWD constructed were difficult to operate. It required two operators, one of which had to hold the device while the heavy weight dropped close to his head. The transportation the device was also troublesome (Bohn, 1989).

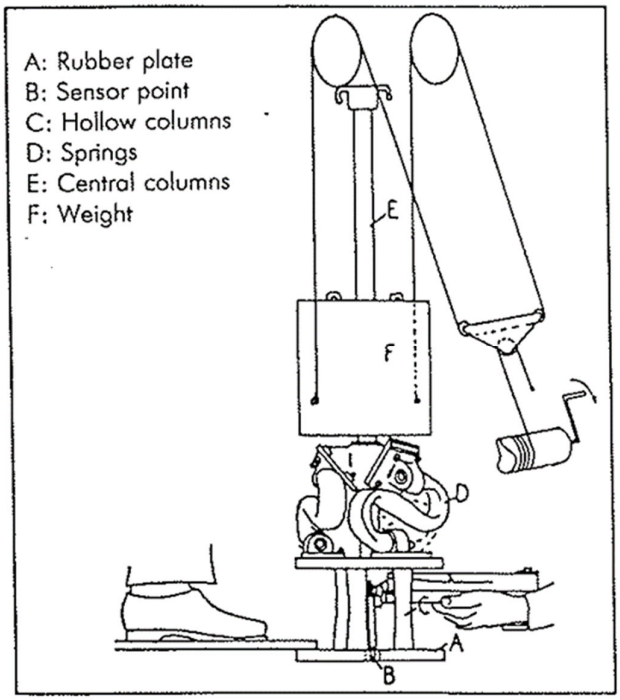

Figure 2.5 – The first Danish Falling Weight (Bohn, 1989)

The first FWD to be commercially available was made my Danish company A/S PhØnix (nowadays Carl Bro) and made debut in 1965. Because of its wide field of application and ease to operate, there are currently multiple manufactures of FWD's (Irwin, 2002):

- Dynatest (Denmark and USA)
- KUAB (Sweden)
- JILS, Foundation Mechanics (USA)
- Carl Bro (Denmark)
- Kamatsu (Japan)

As FWD are gaining experts acceptance, the necessity to share information and experiences of the practice generated user groups such as the Falling Weight Deflectometer User Group (FWDUG) and its European counterpart, EuroFWD.
Although the FWD was designed to be a network level measurement equipment, practical experience revealed its most appropriate usage to be point-to-point at project level measurements (Antonsen & Mork, 2017)

2.2.2 Operation principle

The basic principle behind the deflectometer is a mechanism of hydraulic lifters that elevate a predetermined mass of weights to a certain height then drops. This mass generates a force on impact thought a set of rubber bumpers producing a load cycle equivalent to a vehicle wheel in normal traffic speeds. The FWD is highly mobile when compared to other type of static and rolling wheel equipment giving administration entities the flexibility necessary to perform surveys in a broad area in limited time. Given its operation principles and a computerized user interface, the FWD has been recognized as the preferred method to perform deflection measurements.

Prior to testing the pavement's load-carrying capacity it is necessary to specify parameters on which the test is to be conducted, essentially to define the test protocol: test location and its structural constitution, load force values, loading plate diameter, geophone positions and pavement surface temperature.

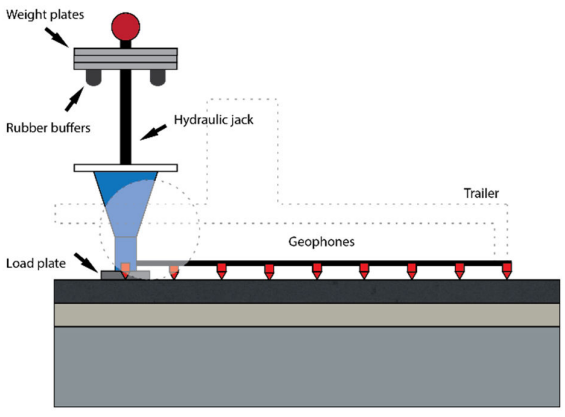

Figure 2.6 - FWD detailed overview

2.2.3 Load force

The load force necessary for a pavement test depends mainly on the pavement type (flexible or rigid). Higher load produces more impulse on the pavement and thus higher deflection readings. Depending on the pavement constitution, a rigid pavement will require higher load to generate a deflection value within the system's geophone resolution and range. The FWD has modular loading plates, each weighting a certain quantity and in conjunction can generate the intended load. Most recent computerized FWD systems can self-calibrate its operation upon deployment and automatically choose the correct drop height to make the setup force. The capable load range of FWD is between 7 kN and up to 240 kN. For heavier loads, specifically for airfield pavements testing, there are a variant called the Heavy Weight Deflectometer (HWD) designed to cope with a wider load range to effectively simulate the pavement impulse of heavy wide body commercial aircrafts such as the Boeing 777 or the Airbus A380. These HWD can obtain deflection measurements of loads ranging from 40 kN to 350 kN.

2.2.4 Dampening system

The weight dropping mechanism generates a pulse of force that is transmitted to the ground through a dampening system. This load pulse is comparable to the action of a wheel axle on the pavement. The load pulse transmitted to the pavement is shaped as a half-sine curve similar to the actual impulse produced by a wheel axle. During the development of the FWD system, the rubber bumpers acting as dampers for the falling weight plates were identified as determinant to the force curve shape generated (Bohn, 1989). For these reason, the configuration of weight plates and the number rubber buffer in the system may significantly change the shape of the load pulse generated and, consequently, the value of load pulse time and the resulting deflections.

Figure 2.7 – Realistic FWD loading model (Madsen & Levenberg, 2017)

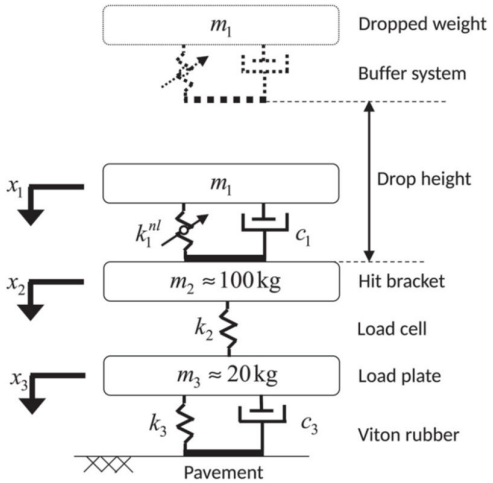

The dampening system comprises from rubber materials which means that its behavior change depending on the conditions tested on: temperature, load level and even the buffer physical shape change the spring effect "constant". It is therefore expected that different FWD equipment display different buffer responses and thus, generate different load pulses resulting in different deflection measurements (Van Gurp, 1995).

The bottom load plate constitutes the main interface between the FWD loading mechanism and the pavement surface. This component main function is to guarantee an even distribution of force to the pavement by providing an adequate seating on the surface. The FWD equipment usually includes several plates with different dimensions. Loading plates with 30 cm diameter is considered the most appropriate dimension to reproduce the footprint of a truck wheel acting on the pavement surface.

2.2.5 Load pulse

Load pulse is the time that the FWD takes to fully deploy the impulse load on to the pavement. This force cycle is configured to be shaped as a sine curve and the duration and magnitude of the force applied by the FWD is representative of the load pulse that would be induced by a vehicle in movement (Garg, 2002). The load pulse is a parameter measured in milliseconds and can vary between 25 and 60 ms, depending on what kind of wheel axle is being simulated.

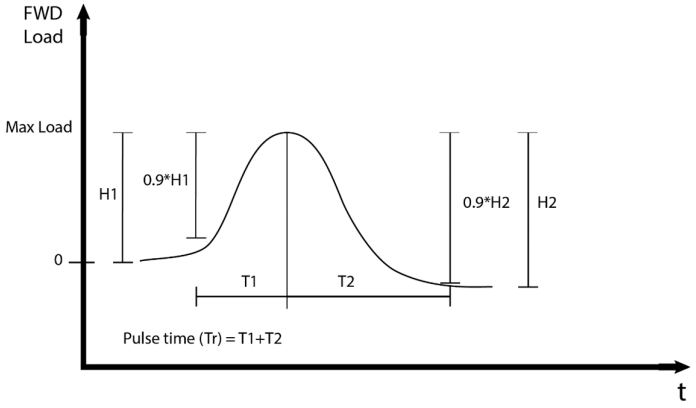

Figure 2.8 - Pulse time definition (FAA/SRA International, 2014)

Pulse time is particularly important to control in multi-layered pavements that are flexible, cohesive soils or saturated soils, for it may influence to some degree the obtained deflection measurements. Lukanen (1992) studied thoroughly the effects between different combinations of buffer configurations, and even concluded that load pulses do not follow exactly a haversine shape but instead the rise and drop are asymmetric, with buffer cross-section configuration having influence on the resulting pulse shape. Madsen et al (2017) produced a comprehensive test studying the influence of FWD load-time history on backcalculated deflection. Several case scenarios are presented to study the effects (Figure 2.9): (a) drop height variation, (b) dropped mass variation.

In the case of a varying drop height, while maintaining constant the buffer configuration and the dropped mass, the FWD generates an increased peak load and shortening of the pulse length (effectively a narrower pulse curve). As mass increases while maintaining a constant drop height and buffer configuration, both peak load and pulse duration also increase producing a wider pulse curve.

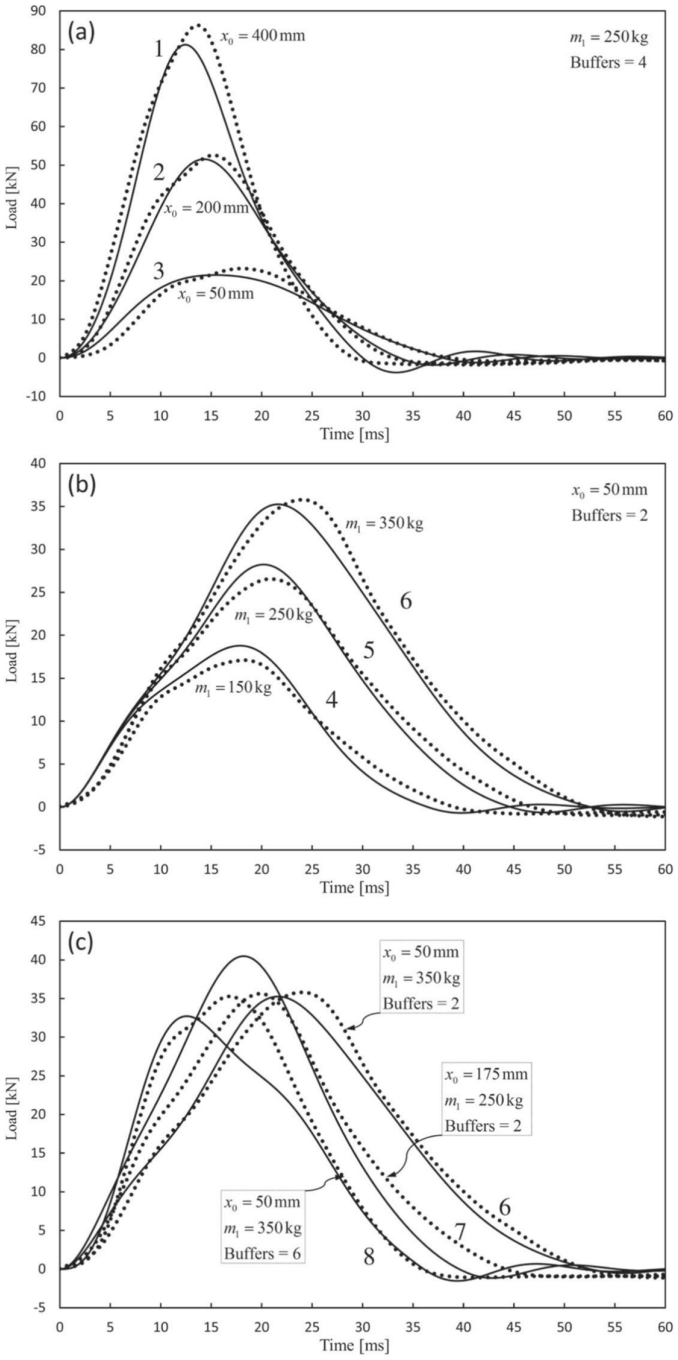

Figure 2.9 – Measured (dotted) and modeled (solid line) FWD load-time histories (Madsen & Levenberg, 2017)

2.2.6 Geophones

The FWD can have up to 9 geophones attached to the trailer. These sensors are evenly spaced and directed radially away from the center of impact. The geophones are transducers that capture minute surface displacements (analog signals) and convert them to electronic signals enabling

computers to record even small amount of surface movement. FWD may use one of two types of displacement measuring device, Geophones (Seismic Velocity Transducers) that measure movement velocity and convert the signal into deflections, or, Seismometers (Seismic Displacement Transducer) that directly measure surface deflection. The resulting array of deflection measurement from the impact center produce a graph named the Deflection Basin which helps visualize the structural capacity of the layers below surface (Figure 2.10).

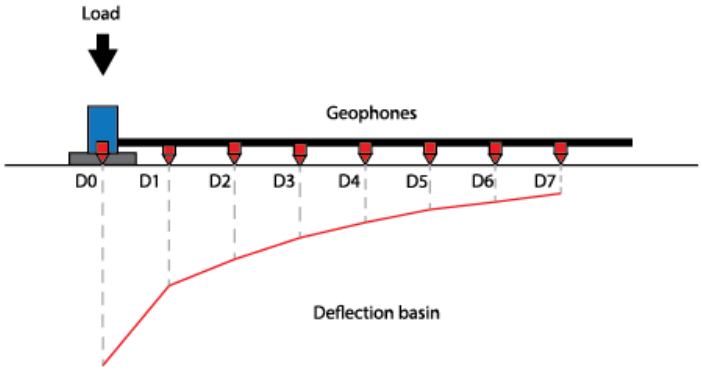

Figure 2.10 - Deflection basin

2.3 Backcalculation

2.3.1 Introduction

The FWD is currently the standard impact loading device capable of simulating pavement deflections comparable to road traffic. By using linear elastic layer theory in the inverse order, the backcalculation process consists in obtaining a estimated deflection basin that matches the measured deflection basin. Irwin, (2002) conducts a thorough review of some BC models that are currently in use. Backcalculation has been viable because of several pavement engineering achievements since mid-twentieth century:

- Discovery that pavement resistance and deflection are related so that strong pavements have small deflection and weak pavements have larger deflections (1935-1960);
- Development of mechanistic theories that relate fundamental materials properties to the inner forces and deflections in a layered pavement system (1940-1970);
- Development of accurate, easy to use and economical equipment systems to measure pavement deflections (1955-1980);
- Desktop computing (1975)

Pavement engineering common practice assumes linear elastic multilayered models under a constant set of parameters: a static load, elastic modulus of each layer, the Poisson's ratios, and layer thickness. As a simplification artifice, it is also assumed that the layers are homogeneous and evenly thick throughout its length, which is not generally the case.

2.3.2 Principles and complexity

Classical BC process starts with an assumed set of initial (seed) layer moduli values to initiate the iterative process with the objective to minimize the discrepancy between the calculated and the measured deflections. The seed modulus is used to compute deflection values that are compared to the measured deflection. The accuracy of the inverse analysis depends on the assumed seed modulus, with different seed values resulting in different backcalculated deflection values, which in turn, leads to different pavement designs.

The backcalculated elastic moduli should minimize the objective function, RMSE (Root Mean Square Error), which represents the distance between the calculated deflections and the measured ones:

$$\mathrm{RMSE}\ (\%) = \sqrt{\frac{1}{n} \times \sum_{i=1}^{n} \left(\frac{d_{ci} - d_{mi}}{d_{mi}}\right)^2} \times 100 \qquad (2.1)$$

Where:
n - total number of deflectometer stations,
d_{ci} - computed deflection value,
d_{mi} - measured deflection value.

Various authors (Irwin, 2002 and Alkasawneh, 2007) consider RMSE values between 1% to 3% to reflect acceptably accurate estimates, but even with low error values resulting layer modulus may not necessarily be the “correct” one. In contrast, high RMS (>4%) might indicate that there are problems with the assumed multi-layer pavement model. Due to the multimodal nature of the classical BC search space where multiple local minimum solutions exist, reaching a local minimum will result in an “inaccurate” pavement moduli which can be up to twice the accurate value (Alkasawneh, 2007). The inverse analysis problem is complex and classical BC approaches are far from being efficient and easy to perform. During the backcalculation process, several topics need special attention (Correia, 2014):

- Seed moduli

Analysis with different seed moduli may return different results. For these reason, it is best to select seed moduli accordingly to the known layer configuration prior to the start of the analysis, thus solution conversion is optimized.

Table 2.2 - Common elastic moduli values (Estradas de Portugal, 1995)

Layer	Elastic Modulus [MPa]
Asphalt concrete	7000 – 9000 (T=15ºC) 5000 – 6000 (T=20ºC) 3000 – 4000 (T=25ºC)
Asphalt concrete (cracked)	500 – 1000
Concrete cement	10000 - 20000
Cement Bound Material	1000 – 5000
Granular base material	150 – 300
Granular sub-base material	100 – 200
Soil	60 – 100

- Thin layers

Multilayer elastic theory simulation software has difficulties computing effects to layers with thickness bellow 5 cm. Usually situated on top layers, practice suggest aggregating such thin layers with all other asphalt concrete layers in the BC software. This issue relates to the difficulty for the software to compute layer stiffness effects in these layers resulting in an unresponsive model.

- Rigid layers

Rigid layers constitute an artifice input to the pavement model as the bottom layer. In the backcalculation software, the foundation layers is substituted by a rigid layer (high stiffness) which behaves as a limit to the model for deflection calculation. Surface deflections are a sum of deformations from underlying layer materials (Rohde & Scullion, 1990). In consequence, when assuming a rigid layer substituting the subgrade, the deflection measured in the center of the load deployment will lack the deflection contribution from the elastic subgrade.

- Layer thicknesses

In a bearing capacity assessment situation, layer thicknesses are parameters that may not be always available either for missing initial designs or lack of historical records of the infrastructure altogether. In these cases, it is possible to resort to site coring, a kind of destructive test, to allow a better access to the layer composition underneath the surface. Ground penetrating radar (GPR) is a nondestructive alternative, although somewhat less reliable. The GPR generates pulses that are conducted through the materials and reflects on layer interfaces thus estimating layer thicknesses that present distinct wave transmission behaviors. It is also for these reason that this equipment is unreliable for pavement model with consecutive similar layer materials as it cannot distinguish layers that present similar composition, therefore not presenting evident interface threshold.

- Interdependency between subgrade and unbound aggregate layers

Successive layers of unbound aggregate layers tend to increase its stiffness towards the surface layers (Salt & Stevens, 2007). In practice, the unbound pavement layers do not have any intrinsic moduli as asphalt bound materials have, and as such, it effectively depends in the stiffness of the materials present in the underlying materials. As an example, an unbound aggregate layer cannot be successfully compacted over a softer subgrade. The resulting consequence would be fracturing of the unbound layer with the appearance of horizontal tensile stresses due to traffic. Dormon & Metcalf (1965) proposed equation 2.2 for the relationship between successive unbound layer interfaces:

$$\frac{E_g}{E_S} = 0.2 \times h_g^{0.45} \qquad (2.2)$$

Where:
E_g – Elastic modulus of granular layer,
E_S – elastic modulus of subgrade layer,
h_g – Granular layer thickness.

Various researchers (Brown & Pappin, 1981; Claessen et al, 1977) through more rigorous analysis concluded that the ratio from equation 2.3 would be valid in the interval between:

$$1.5 < \frac{E_g}{E_S} < 7.5 \quad (2.3)$$

In respect to backcalculation software, by default, it only optimizes the RMSE of resulting deflection graph and may ignore the necessity to reflect the ratio between overlaying unbound layers.

- Non-linear material layer

Non-linear material present increased elastic modulus when further away from the point of load deployment. As such, when performing backcalculations on non-linear layers (subgrade layer) while assuming a linear behavior, the resulting modulus can be very different and far from the real elastic modulus. This issue can also propagate negatively in the other overlaying materials estimated moduli as the model tend to compensate producing unreal results (Correia, 2014)

- Temperature

Asphalt concrete layers are susceptible to stiffness variation depending on ambient temperature and frequency. During pavement testing, this viscoelastic material may present different temperatures in different testing sections or even within the layer itself. Dormon & Metcalf (1965) conclude that as the asphalt layer becomes hot, it become less rigid and thus offer less protection for underlying layers, increasing strains in the subgrade. The pavement deflection measurements being dependent from temperature and frequency require that the backcalculated modulus be corrected to a reference temperature (Fernando et al, 2001). Flores et al. (2017) develop a study for correction models for FWD backcalculated moduli relating to frequency and temperature factors. It is concluded that reference frequency and temperature closer to field frequency and temperature achieves more accurate modulus estimated values (Figure 2.11).

Pais & Pereira (2017) also present a study to develop a model to adjust FWD deflections for temperature variations. The author defines a concept of “deflection ratio” which relates the measured deflection at a given temperature and the deflection for a reference temperature at 20ºC. Since the stiffness is dependent of the temperature, the magnitude of modulus variation is resumed in the following table (Table 2.3).

Table 2.3 – Stiffness modulus for the asphalt layer (Pais & Pereira, 2017)

Temperature [ºC]	Stiffness modulus [MPa]
-10	17500
0	13600
10	9700
20	5800
25	3850
30	1900

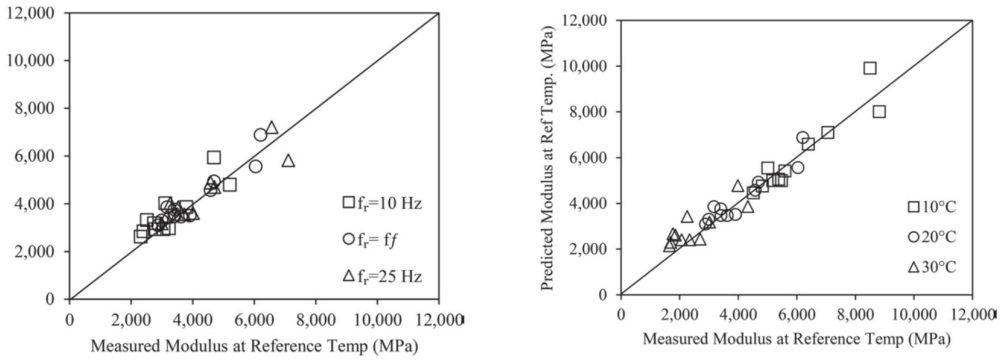

a) Frequency

b) Temperature

Figure 2.11 - Evaluation of the effect of frequency and of temperature to the proposed correction model (Flores et al., 2017)

Simultaneously to the pavement layer temperature influence in the backcalculation process, other temperature sensitive components must be accounted for: the equipment operation optimal temperature and mainly the air temperature that conditions the buffer system's rubber material behavior.

- High frequency disturbance

In the process of FWD testing, the interaction between the set of rubber buffers and the dropped weight may cause load pulse shape distortions (Sorensen, 1993; Van Gurp, 1995). The phenomenon is thought to be due to non-linearity, damping, and temperature dependency of the material properties of both the rubber buffers and the rubber pad under the loading plate and also the pavement material itself. The pavement top layer and the subgrade present some degree of mass and damping, thus reacting as a natural filter to the high frequency component of the impulse loads as it cannot respond as quickly to the high frequencies of the load. Backcalculation process with distorted peak values of load time history and deflection time histories may result in incorrect estimated results (Figure 2.12).

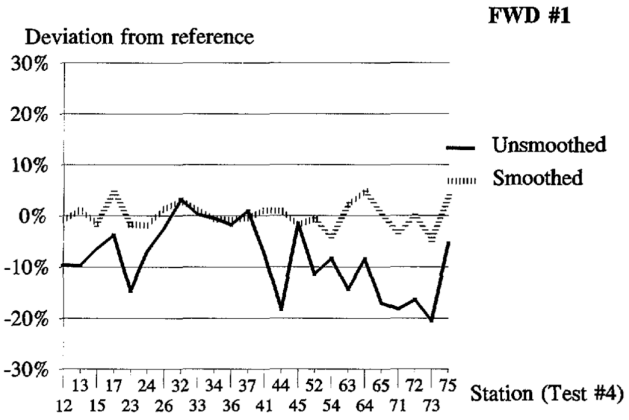

Figure 2.12 - Effect of smoothing on deflections of FWD (Van Gurp, 1995)

Sorensen (1993) concluded that distorted pulses may have its biggest component above 60 Hz frequencies. Pavements, in turn, do not respond to frequencies above 60 Hz. Figure 2.13 shows a principle diagram of a frequency spectrum of the half-sine pulses with a duration of 25 and 50 milliseconds. It is seen that the bulk contribution to the spectrum belongs to the lower frequencies, and above 60 Hz, the contribution is negligible. FWD manufacturers may include a frequency cut-off function for smoothing load and deflection pulses to obtain more precise data. The smoothing function actively reduces peak load values eliminating the high frequency component of the load pulse (Van Gurp, 1995). This contributes to a lower backcalculated stiffness value when compared to unsmoothed data.

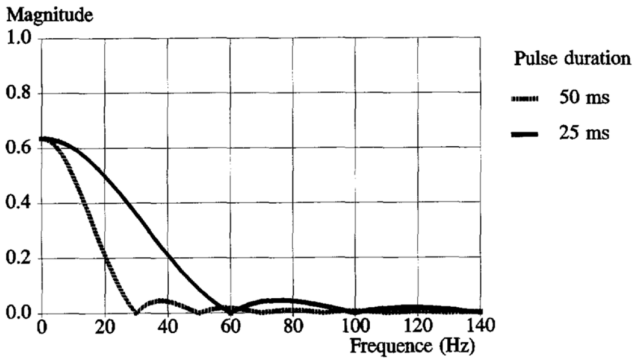

Figure 2.13 - Fourier transform of two half-sine shock pulses (Van Gurp, 1995)

The form of these signals is dependent of the FWD manufacturer and the specific model. It is common practice by FWD manufacturers to not disclose how exactly these signals are interpreted.

2.3.3 Classical backcalculation methods

Linear elastic multilayer model software available, such as BISTRO, BISAR (Shell) or ELSYM 5 (Chevron) are used in the process of manual backcalculation. These software's can calculate the model's deflection response to a given force load and the assumed parameters such as: layer thickness, Poisson's ratio, and the seed moduli. The process is iterative and may be time consuming depending on the assumed seed moduli. This methodology was adopted as basis for Chapter 4 analysis.

2.3.4 Modern optimization techniques

Over time, researchers have been exposing limitations of classical BC approach. The necessity for initial proprieties assumptions may result in obtaining a local minimum solution. In this section, we present some researchers propositions comparing classical BC methods to alternate more efficient optimization methods:

Genetics Algorithms is presented as a superior method to optimize functions of large search space. With this algorithm, the necessary parameters are encoded in binary code and for this reason the parameters themselves are not used throughout the process. These strings are grouped in populations and searched simultaneously rather than point by point (Goldberg, 1989).

This method takes advantage of the simultaneous search for optimal solutions increasing the probability of finding it. Previous population of strings is used to create a new one using genetic algorithms and the suitability (fitness) of the solutions is tested by the objective function before proceeding to the next repetition of the process (Alkasawneh, 2007).

Artificial Neural Networks (ANN) is a computerized network of algorithms that can adapt and learn from previous calculations and error corrections. The benefit of a fully trained artificial neural network is its ability to compute simultaneously elastic moduli, thicknesses and the Poisson's ratios. The only issue is referred to the learning process that takes a long time until it is able to solve any complex problem. Rakesh, (2006) successfully proved that ANN computation time could reduce Genetic Algorithm computation time by 97% while maintaining the robustness and achieving global solutions.

Levy Ant Colony Optimization Algorithm is a heuristic algorithm applied to backcalculation of pavement moduli. Fileccia Scimemi, (2016) propose this heuristic approach to remove assumptions out of the classical BC process. It is described that without these assumptions the proposed algorithm is able to freely explore solutions giving better quality solutions even to increasing complex problems. ACO is inspired by ant foraging behavior. The objective function reaches the global minimum solution following steps of preferable choices just like ants would when navigating outside their colony following fellow ant pheromones.

Garbowski & Pożarycki (2016) produced a comparison research between classical "Single-level" backcalculation algorithm and Multi-level Backcalculation Algorithm. The classical BC is highly dependent of seed moduli and the assumption a constant value for layer thickness. It is claimed that wrongly assumed thicknesses will in turn make the algorithm converge to wrong elastic modulus values. The proposed method is capable of simultaneously converge the thickness parameter (RMSE <1%) and sub sequentially update itself to improve the estimates of elastic moduli from the various layers in the model.

2.4 FWD Accuracy

The FWD is used to assess pavement bearing capacity (Bush & Baladi, 1989; Quintus et al, 1994; Tayabji and Tayabji & Lukanen, 2000) by measuring surface deflections and, through a backanalysis process, estimate the elastic moduli of underlying layer, which in turn, indirectly assesses the remaining serviceable life span.

Although FWD are commonly requested by administrations for routine campaigns, several authors (Van Gurp, 1991 and Murphy, 1998) have given evidence of lack of reproducibility between a FWD fleets. Researchers Rocha et al (2004) presented a thorough literature review on the accuracy and precision of FWD. The main possible sources of uncertainty in FWD measurements most commonly reported in the literature are related to its buffers and the pavement stiffness. The shape, size, age and stiffness of rubber buffers impact the peak load, the rise time and the load pulse shape, and in consequence the magnitude of the deflections (Chen et al, 1999; Lukanen, 1992). The impact of buffers characteristics on deflections also depends on the pavement structure and it is mainly important in the case of weaker pavements (Chen et al., 1999). Van Gurp (1995) also underlines the difficulty to achieve machine-independent results. Having calibrated load cells and calibrated deflection sensor does not offset the different equipment characteristics, such as, rubber buffers shape and hardness, the thickness and quality of rubber pad under the load plate, the type of deflection sensor, sensor

positioning in the frame, and other factors that impact the load pulse shapes and deflection readings. FWD time histories produced by one equipment are different for another FWD, producing different peak force values. This implies that data collected from different FWD are not intercomparable, even in the case of fully calibrated equipment.

Leiva-Villacorta (2012) reported that FWD impact load testing performed at the National Center for Asphalt Institute (NCAT) test track generated impact loads more representative of a truck travelling at 120mph (193 km/h), an unrealistic traffic speed.

Irwin (2002), also presents a summary of the three main types of FWD errors:

- Seating errors are mechanical errors derived from each time the FWD deploys to measure surface deflections. Debris or irregularity from pavement damage can influence these kinds of error. This error can be eliminated by performing up to two sequential drops to guarantee the correct LVT sensors seating.
- Systematic errors, in the case of a measuring equipment, are related to factors that consistently produce readings too large or to small in relation to the reference values. The concepts behind these symptoms are trueness and bias. This can be eliminated from FWD measurements by routinely calibrating the equipment.
- Random errors are related to the varying values of consecutive results. These errors are derived from the analog-digital signal conversion from each LVT sensor. An effective way to reduce this error to a minimum is by averaging the measured results. Each manufacturer encodes the analog displacement signal conversion to digital signal differently to be interpreted by computer software and therefore is not possible to standardize this process. It is these random errors that contribute to the repeatability and reproducibility issues in study and both included in the study of the FWD precision.

Uncertainty is usually expressed either in terms of standard deviation of mean (σ_m) or in terms of a percentage (ε).

ASTM D4694 and ASTM D4695 are standard documents related to deflection measurements with FWD. These documents refer that precision is a function of both the characteristics of the pavement and the used device. However, several studies were already performed with different devices to obtain FWD precision data (Van Gurp, 1991; Choubane et al, 2006; Bentsen et al, 1989; Rocha et al, 2001 and 2004). Nevertheless, more studies are needed to improve the knowledge about FWD precision and the uncertainty evaluation is still a gap of the literature.

2.5 Summary

Road administration focus shift towards asset management contributed to the development of increasingly efficient Pavement Management System methodologies. By routinely performing network level pavement testing campaigns, road pavement conditions are periodically logged in PMS database allowing for critical road sections to be identified and interventions planned.

Non-destructive testing procedures gained acceptance for routine pavement testing for being considered the most efficient and less intrusive in normal traffic conditions. Surface distress detection and bearing capacity assessment are possible with NDT equipment. Network level campaigns are most commonly performed with surface distress assessment equipment due to technical inefficiency of currently available bearing capacity measuring equipment such as the

Benkelman, the Curviamètre or the FWD (Antonsen & Mork, 2017; Santinho Horta et al., 2011). Bearing capacity assessment is therefore confined to point-to-point measurement in critical sections previously identified by surface distress evidence (Zofka et al, 2017).

The Falling Weight Deflectometer is considered the standard deflection measuring equipment. It is a stationary impact load type deflectometer (Čičković, 2017) with a hydraulic mechanism that elevates a conjunction of weight plate and drops over a system of rubber buffers and load plates seating on the surface. The provoked vertical pavement displacement (deflection) is recorded by sensors stationed at fixed distances radially away from the impact point. These sensors are Linear Differential Vertical Transducers (LDVT) which contain a moving permanent magnet that induces a voltage signal in the encapsulated coil. The digital signal produced is converted into data accessible through FWD bespoke software. The FWD has the particularity of being relatively mobile and has the particularity of being able to produce a complete deflection basin from underlying layers, therefore, capable of generating data accurate enough for backcalculating layer properties (Andersen et al., 2017).

Several authors have studied FWD limitations mainly due to concerns of lack of reproducibility between individual equipment (Murphy, 1998; Van Gurp, 1991). The identified sources of non-reproducibility derive from multiple factors involved in the testing process. To some degree, not all source can be controlled and mitigated. The load pulse shape is dependent of the buffer system geometry and alignment, but also influenced by the pavement and subgrade constituting material type. The load pulse time duration is currently determined by factory default, except for the KUAB FWD which is designed with longer loading time. The manufacturer's technique deflection signals conversion also influences the quality of deflection data. High frequency disturbance can contribute to distortion of the pulse load shape and the deflection pulse. Comparing distorted peak values of the load time history and deflection time histories may affect backcalculation estimated results. It is therefore recommended, when available, to enable smoothing filter function to cut off frequencies above 60 Hz (Sorensen, 1993; Van Gurp, 1995).

Backcalculation is a process in which pavement stiffness modulus is estimated by reverse calculations possible from deflection data. Irwin, (2002) conducts a thorough review of some BC models that are currently in use. Various authors (Irwin, 2002 and Alkasawneh, 2007) consider RMSE values between 1% to 3% to reflect acceptably accurate estimates, but even so resulting layer modulus may not necessarily be the "correct" one. High RMS (>4%) might indicate that there are problems with the assumed multi-layer pavement model. Due to the multimodal nature of the classical BC search space where multiple local minimum solutions exist, a local minimum will result in an "inaccurate" pavement moduli that can be up to twice the accurate value (Alkasawneh, 2007). The inverse analysis problem is complex and classical BC approaches are far from being efficient and easy to perform.

3 Proficiency Test

3.1 Introduction

The following section describes a field trial aimed to determine the state of the art of FWD practice in Portugal. This section was inspired by the necessity to bring together a fleet of commercially available FWD equipment and, through a proficiency test scheme (PTS) assess how the participants would perform in an interlaboratory comparison. All the participants were well experienced operators of FWD in Portugal, each having provided pavement surveys and consultancy services for both road and airport administrations, in routine tests and tenders for pavement evaluation. This field trial constituted a rare opportunity to have firsthand experience and understand the behaviors of different FWD equipment from various manufactures, while joining experienced FWD operators to exchange knowledge and provide valuable experimental data. This PTS event was organized under RELACRE management and the test data was disclosed with permission.

This section also serves as preparation for Chapter 4 which aims to analytically study repeatability and reproducibility (ISO, 1994b) of this type of equipment. With the data results, the equipment uncertainty will be related to how it may in turn influence the backcalculated pavement stiffness modulus. The final objective is to assess how would the involved errors and discrepancies from this standardized process can influence the backcalculated layer moduli, thus leading to incorrect project designs.

3.2 Equipment

Invitations to participate in the PTS (ISO, 2010) were sent to several portuguese FWD owner entities in the public sector. From the invitations sent out, three entities showed availability to partake the experiment.

In hope that our devised scheme would be as faithful as possible to a real-world scenario, the testing was conducted by letting each participant team perform their usual routines while performing the FWD drops and measuring deflections. This would ensure that the obtained results would be faithful to the obtained in an actual road maintenance campaign.

The three participating entities brought their FWD equipment, each with their respective technical specification resumed in Table 3.1:

- Carl Bro PRI 2100 FWD trailer (Figure 3.1a)
- KUAB 240 HWD trailer (Figure 3.1b)
- Dynatest 8002 FWD trailer (Figure 3.1c)

Table 3.1 - Main specifications of FWD equipment

Manufacturer	Carl Bro	KUAB	Dynatest
Model	Carl Bro PRI 2100	KUAB 240	Dynatest 8002
Year of acquisition	(*)	2004	2002
Load range [kN]	7-250	30– 240	7-120
Load pulse time [milliseconds]	20-30	30	20-30
Diameter of load plate [cm]	30 and 45	30 and 45	30 and 45
Type of deflection sensors	Seismometers	Geophones	Geophones
Deflection sensor range [μm]	2.2	(*)	(*)
Relative accuracy of deflection sensors	1 μm ± 2%	(*)	2 μm ± 2%

(*) Not available

a) Carl Bro

b) KUAB

c) Dynatest

Figure 3.1 - FWD equipment

From this group of equipment, there were several particularities that should be noted:

- Both Carl Bro and Dynatest FWD were fully computerized models and were able to automatically record peak load values and it respective pulse time history. On the other hand, KUAB HWD belonged to older generation equipment lacking the capability to self-calibrate the optimal drop height for target force load and it also could not measure pulse times. To counter this issue, and to follow test protocol nonetheless, KUAB operators had to previously simulate FWD drops and manually set the drop heights at which would generate the necessary force load to use during the PTS.
- All equipment had the ability to interchange weight plates to achieve required nominal loads and had the ability to physically change the buffer configuration as required.

3.3 Test facility

FWD tests were conducted on December 6, 2016. In total, there were two test sites (Table 3.2), test site 1 with a flexible pavement and test site 2 with a rigid pavement. The pavement was evenly regular and did not show signs of damage. Its layer composition and thicknesses were determined by coring a sample in a nearby area. The test site 2 was inside an aircraft hangar. At this location, the layer composition was obtained by reviewing the initial designs of the building as it was not possible to coring.

Figure 3.2 – Test site 1

Table 3.2 – Characteristics of the test sites

Site	Pavement	Layer	Material	Thickness [cm]
1	Asphalt concrete	Surface	Asphalt concrete	5
		Base	UGM (1)	20
		Subgrade	Soil-cement	15
			Sandy soil	15
2	Concrete	Surface	Concrete slab	20
		Base	Paving stones	12
		Subgrade	Soil-cement	(2)
			Sandy soil	(2)

(1) - Unbound granular material; (2) - Unknown

3.4 Testing procedure

The FWD tests were performed according the method described in ASTM D4694 (ASTM, 2009) and ASTM D4695 (ASTM, 2008). For the PTS, each party has previously been informed about the test protocol and was fully briefed about the proceedings to be performed (see Appendix I).

Before beginning with the PTS, the exact location for placement of the load plate was marked on the pavement. The direction of alignment of the geophones was also determined to guarantee test consistency between equipment. The test would consist in five consecutive drops: the initial two drops as adjustment drops to correctly settle the geophones, followed by another three drops that would enter for the data analysis process.

The deflections were measured by sensors in 8 points located at different distances from the center of the load plate: 0, 30, 45, 60, 90, 120, 150, and 180 cm. The number of available sensors depends on the manufacturer and equipment model, and most equipment allows for the sensors to be repositioned as needed. As a result, the sensor spacing will depend on the number of available sensors and the length of the sensor bar. However, all the three devices have used the same sensors configuration. Peak of deflection at each location resulting from the force pulse was recorded in micrometers [μm] by two types of deflection transducers (see Table 3.1): seismic velocity transducer (geophones) and seismic displacement transducers (seismometers). Each test deflections measured by the sensors together creates the deflection basin for pavement model.

Table 3.3 – Test protocol

Site	Load peak [kN]	Deflection sensors distance [cm]	Load plate diameter [cm]
1	65, 90	0, 30, 45, 60, 90, 120, 150, 180	30
2	90		

Taking turns, the FWD were stationed on the exact test location and the geophones aligned with the defined direction. Following the test protocol, the sequence of events was as described in Table 3.4. After each drop test, deflection measurement was recorded and exported to confidential files and later sent to the organization team.

Table 3.4 - Sequence of events

Phase	Action
Preparation	Alignment of the FWD load plate with ground mark with correct orientation of the geophones
	Load weight plates necessary to generate forces of 65 kN or 90 kN
	Measure surface and air temperature with laser thermometer
	Deploy geophones on the pavement and assure correct sensor adhesion to pavement with first two drops
Test	Perform a series of three drops
	Recording peak load and load time history to a file
	Retract geophones to end test

3.5 Results

After each drop sequence, the deflection readings were recorded and confidentially stored by the test organizer. Back in the laboratory, the data was analyzed as described in Chapter 4. The deflection values were firstly normalized to their nominal load values. The averaged deflection values for each FWD is shown in Figure 3.3 (a, b, c). Observing the charts, FWD 1 produced data consistently shifted from the rest of the sample. This occurrence may be related to the fact that the FWD have different kind of geophone or because the equipment is off calibrated, but in this case, FWD 1 provider did have proof that their equipment was recently calibrated by manufacturer. In both case, the deflection curve shape is still consistent with the rest of the participants although shifted from the rest of the results measuring significantly lower deflections. The recorded load pulse time was within the interval of 17 to 28 milliseconds, slightly off from the manufacturer specified 25-30 milliseconds pulse time.

Separately from the PTS, and following recommendations from Madsen & Levenberg (2017), it was urgent to understand the effects of different load pulses in resulting deflection measurements.. In a FWD drop test there are several mechanical variables that play a part in the process of impulse generation. A combination of 3 different variables such as drop weight, drop height and buffer setting will determine the force generated and also the load pulse shape. A FWD was selected to put in practice a study of this interaction. The number of weight plates was changed in between test rounds thus forcing change of the variables dropped weight and drop height, while maintaining the nominal force output to 65 kN and 90 kN. The buffet configuration was maintained constant at time due to technical limitation in changing the buffer setting. To maintain the peak load value constant, the FWD performed a series of drops while by automatically adjusting its drop height per each load weight setting. Between each round, the number of weight plates were changed from 3 weight plates, 5 weight plates and to a maximum of 7 weight plates. The results (Figure 3.3d) demonstrate that the load pulse time increases with the number of weight plates while resulting deflection measurement also increase (see Appendix I).

To further understand the phenomenon with FWD 1 results, attention was given to its manufacturer instruction manual and the operation proceedings executed while in the PTS. The Smoothing Filter (SF) function was discovered to have been set to a value other than the recommended in the manufacturer's manual (previously set to 150 Hz, instead of the manufacturer recommended 60 Hz). To fully realize the extent of the implications of SF settings, it was proposed to retake FWD 1 tests focusing in obtaining results with various combinations of SF settings. In Appendix II, it is presented the complete study on FWD 1 performance following several test rounds with different SF parameter combinations. It was admitted as reference benchmark SF value of 150 Hz. From the analysis, it was concluded that the initial FWD 1 deflection measurement was to some extent a result of the mistaken SF of 150 Hz, although it was not likely to be the sole reason of such different results. A comparison between newly tested deflections with SF set to 60 and 150 Hz allowed to conclude that the results would differ in 4 to 14% at most.

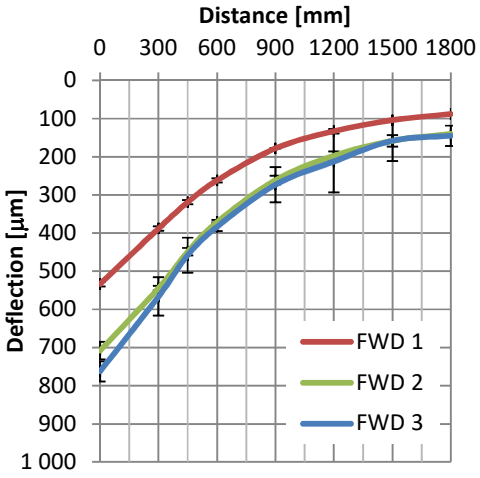

a) 65kN, flexible pavement

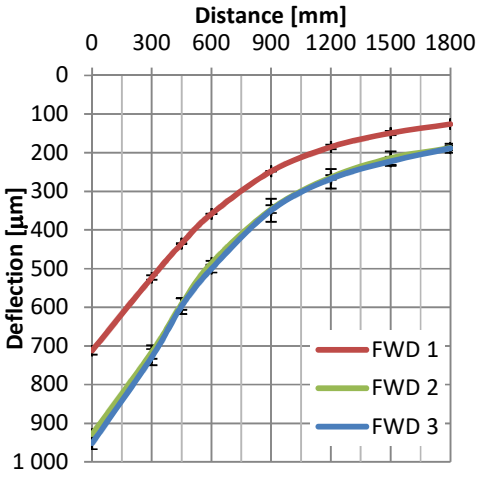

b) 90kN, flexible pavement

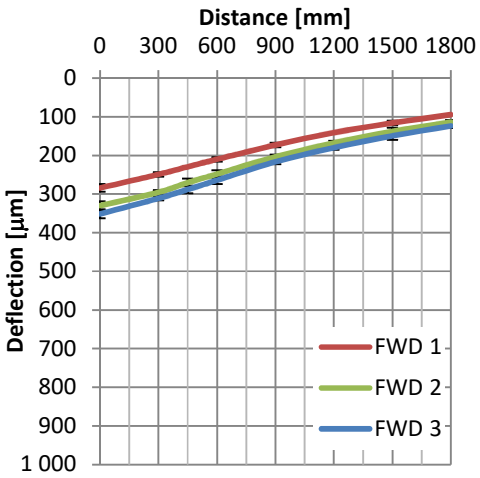

c) 90kN, rigid pavement

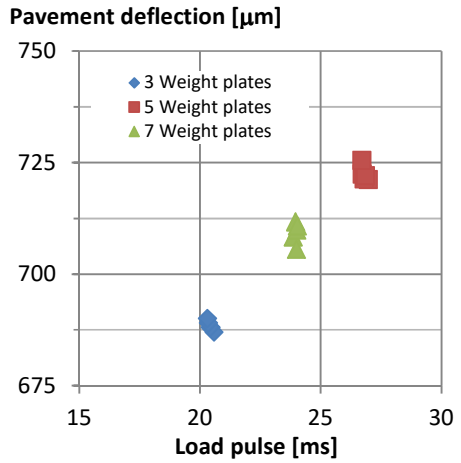

d) Load pulse in relation to deflection values

Figure 3.3 - Deflection charts and Load Pulse influence in deflection measurements

3.6 Summary

This section described the field trial carried out following a Proficiency Test Scheme (ISO, 2010) involving a fleet of Falling Weight Deflectometer (FWD). This test scheme served to acknowledge the state of the art in Portugal and, particularly, within the involved entities.

Three FWD joined the PTS at a testing facility located in portuguese air force base in Alverca. A test protocol was followed with several rounds of drop tests performed (ASTM, 2009). Only the last three drops were considered for later data analysis (ASTM, 2008). It was known beforehand that the load pulse parameter would not be a fully controllable in every equipment prior to the data analysis and as such it would not be possible to standardize all equipment settings with absolute accuracy. The parameter variations between different equipment were considered in the analysis.

The deflection results were plotted in graphs representing complete deflection basins for each FWD measurement in the same marked location. One of the equipment (FWD 1) showed clear bias by recording values consistently shifted by a constant factor in relation to the rest of the test sample. It was later investigated and discovered that technicians had preset the computer software to allow smoothing filtering of the pulse load signals at a frequency different from the recommended in the manufacturer's manual (150 Hz instead of 60 Hz). Further testing was developed in different occasions to understand the differences in the measurements with the various settings for the Smoothing Filter (SF). The SF parameter was set to 0, 60 Hz (default manufacturer setting), 150 Hz and 200 Hz, and deflection test results was measured. For 60 Hz, at peak load force, the results confirms the literature (Sorensen, 1993) with deflection measurement increasing approximately 4% to 14% (see Appendix II). It was concluded that Smoothing Filter parameter error do not justify FWD 1 bias alone.

Separately from the PTS, FWD 1 also performed drop tests while varying weight plate number used in between rounds, aiming to assess the effects on pulse load times and deflection measurements. In Chapter 2 we acknowledged the importance of pulse time influence in FWD tests outcome and intended to have firsthand experience with equipment capable of regulating this parameter. The results were increasing pulse times while deflection itself maintained steady in our test on rigid pavement.

The main conclusions from the experimental research are the following:

- The operators are not fully aware of the large number of parameter variables determining the outcome of the deflection measurements.
- The focus is primarily the peak load values generated by the equipment, the loading plate size and the spacing in between deflection sensors.
- Several other important parameters are overlooked, such as the load pulse time history, the load pulse shape, smoothing filter setting, determined by the rubber buffer configuration, the rubber material properties from each different FWD and the settings in the software regarding high frequency signal disturbances. Load pulse variation effects are particularly significant in case of Asphalt Concrete bound pavements and saturated soils.

4 Data analysis

4.1 Repeatability and reproducibility

Precision of a measurement is related to the distribution of random errors usually expressed in the form of standard deviation. Repeatability and reproducibility analysis of a test sample allows the assessment of precision under repeatability and reproducibility conditions respectively. For this purpose, only the last three load tests results were considered for the analysis. The deflection values were normalized to the nominal load values (Table 3.3). Following standard ISO 5725 (ISO, 1994b), it is assumed that the test result differences existing within-laboratories variance are small amongst laboratories samples. It is necessary to verify the validity of this assumption prior to further analysis through Cochran's test, and then, the Grubb's test, which validates between-laboratory variability (see Appendix III). For each deflection sensor, interlaboratory average of the averages and standard deviation of deflections were calculated. Attending the small standard deviation values, it was applied a factor of amplification of ten times in order to be represented in the deflection charts (Figure 3.3 a,b,c).

As defined by the international standards (ISO, 1994a), *repeatability and reproducibility limits are values less than or equal to which the absolute difference between two test results obtained under repeatability (or reproducibility) conditions may be expected to be within a probability of 95%.* Repeatability and reproducibility is conditioned by equipment differences and other environmental parameters such as the temperature. This study confirmed an acceptable repeatability limit for both types of pavement but, in contrast a high reproducibility limit was obtained in test site 1, mainly due to the FWD 1 device. Attending to the fact that FWD 1 results deviate strongly from FWD 2 and FWD 3, repeatability and reproducibility analysis was performed in two distinctive case scenarios. The first one "N=3", in which results will be calculated considering FWD 1, 2, 3 and, the second case "N=2", calculations will only feature FWD 2, 3.

This analysis results produced plot graphs that illustrate the comparison of repeatability and reproducibility limits. Table 4.1 summarizes the resulting repeatability and reproducibility limit values (r, R). Both are functions of deflection magnitude (D_f) and pavement stiffness (flexible or rigid pavement). As expected, by removing the outlier FWD 1, both repeatability and reproducibility limits improved significantly in the N=2 scenario.

Analyzing Figure 4.1, repeatability limit for both N=3 and N=2 seems to scatter uniformly settle around r=4 and r=2, respectively for Site 1 (flexible pavement) and Site 2 (rigid pavement). Figure 4.2 presents the reproducibility limits with trend lines and their respective expressions. For Site 1, being a flexible pavement, the limit for N=3 increase rapidly when deflection values also increase towards peak values in the center of test impact. Serving as an indicative example, for a given deflection D=300 μm, R=169. This is clearly due to FWD 1 measurements that contribute to such high standard deviation of the mean values, thus presenting such steep slope. With the N=2 scenario, without FWD 1 contribution, reproducibility limits clearly drop to acceptable values and trend line stay almost flat in the entire deflection range. In the same line of example as above, for a D=300 μm, limit is returned as R=13. Same analysis is valid for Site 2 reproducibility limits, although predictably, for rigid pavements, the trend line presents a smaller slope, for given D=300 μm, R=93 (N=3) and R=25 (N=2) (see Appendix III and Appendix IV).

Table 4.1 - Repeatability and reproducibility limits

	Test Site	Repeatability r	Reproducibility R
N=3	Site 1	4	$1.702D_f^{0.864}$ (R^2=0.99)
	Site 2	2	$0.9251D_f^{0.8081}$ (R^2=0.99)
N=2	Site 1	4	$0.1163D_f^{0.8257}$ (R^2=0.37)
	Site 2	2	$0.7906D_f^{0.6042}$ (R^2=0.90)

r – repeatability limit; R reproducibility limit

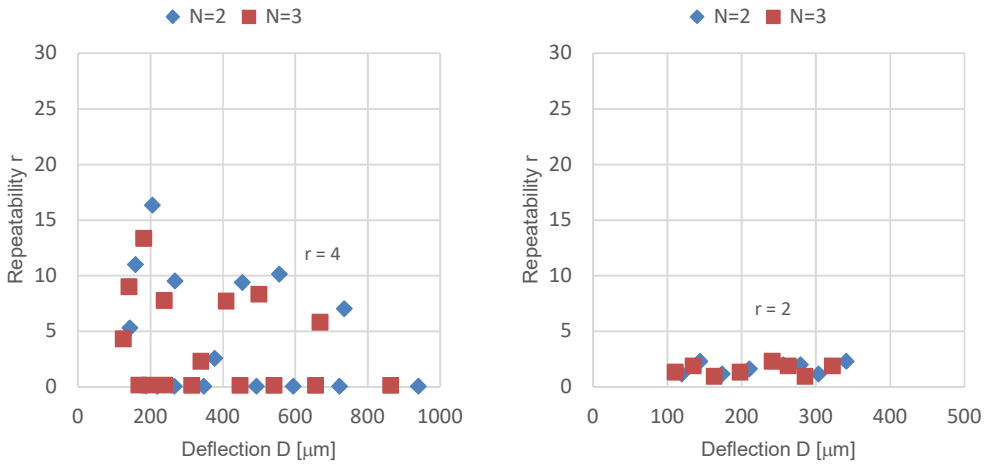

a) Site 1 b) Site 2

Figure 4.1 - Repeatability limits for deflection measurements

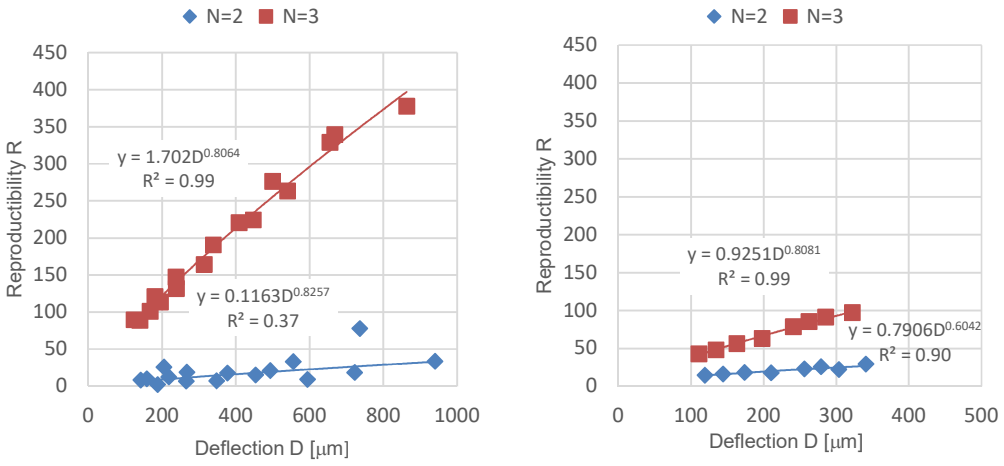

a) Site 1 c) Site 2

Figure 4.2 - Reproducibility limits for deflection measurements

4.2 Uncertainty assessment

This section proceeds with the assessment of the uncertainty presented by the FWD test results.

To study the uncertainty, firstly it was necessary to attain the critical values for this statistical model. From the repeatability and reproducibility analysis, it resulted values for the mean of the means and its respective standard deviation for each geophone position (a total of 8 positions). These data fitted a normal distribution leading to the estimation of the critical values for a normal distribution standard variation of the means with a confidence level of 95%, obtained with equation 4.1. For a confidence level of 95%, the critical value is 1,96 and n=1, as we are calculating critical values for a deflection value at each geophone position.

$$z \times \frac{\sigma}{\sqrt{n}} \tag{4.1}$$

The critical values are resumed in Appendix V. When comparing with the N=3 case, the critical values are significantly smaller for N=2, representing the case in which a FWD fleet presented satisfactory repeatability and reproducibility. Figure 4.3 presents the graph for the deflection mean of the means values as a function of their respective critical values. The model indicates a good fit (R^2=0.99) mainly from N=3 cases. It is noticeable a positive trend for which the critical value increases with the deflection magnitude. To express this relationship resulted from the PTS experiment, a trend line was plotted and its governing equation will serve as the model behavior rule to calculate critical values for given any deflection.

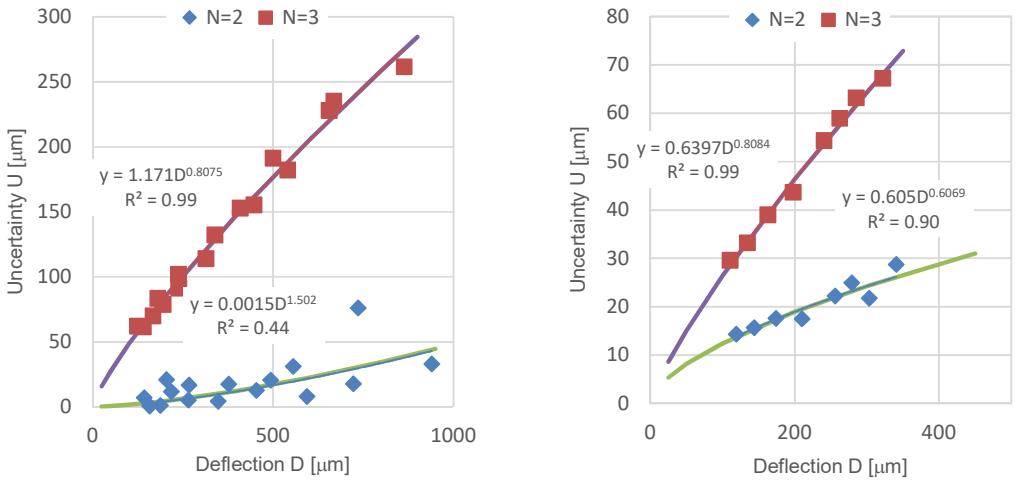

a) Site 1 b) Site 2

Figure 4.3 - Uncertainty of deflection measurements

The equations are resumed as follows:

$$Y = 1.171D^{0.8075} \quad (4.2)$$

$$Y = 0.639D^{0.8064} \quad (4.3)$$

$$Y = 0.0015D^{1.502} \quad (4.4)$$

$$Y = 0.7605D^{0.6089} \quad (4.5)$$

Equation 4.2 describes the critical values obtainable with deflection values for flexible pavements in the case scenario where FWD present acceptable repeatability but lack of reproducibility. Equation 4.3 describes the case scenario where FWD present acceptable repeatability and reproducibility. Equations 4.4 and 4.5 represent the same sequence of case scenarios, respectively, but only for rigid pavements.

4.3 Sensitivity analysis

In this section, a sensitivity analysis is performed using the data obtained from chapter 4.2. The aim is to extrapolate the uncertainty data and apply it in a sensitivity analysis on standardized flexible pavements suggested in the Portuguese pavement design manual, known as MACOPAV (JAE, 1995). These pavement models are used in real world practice by pavement designers and so the results should constitute a close proximation to a real-world application. As the scope of this study is only flexible pavements, the uncertainty critical values will only be obtained through the equation 4.2.

The analysis makes use of standardized flexible pavements models suggested by MACOPAV design manuals. Each pavement model has attributed reference moduli values for each type of layer and finally, through BISAR multilayer elastic linear pavement design software (Shell, 1995), the models deflection basin were calculated.

Several pavement configurations models were selected from the manual (see Appendix VI). The criteria for pavement selection within the manual was to include the most recurrent subgrade classes of pavement, F3 (Figure 4.4) and F2 (Figure 4.5). The other criteria were to study the opposite scenarios of Traffic class, T1 (most traffic) and T6 (less traffic). The resulting pavement selection is presented as follows:

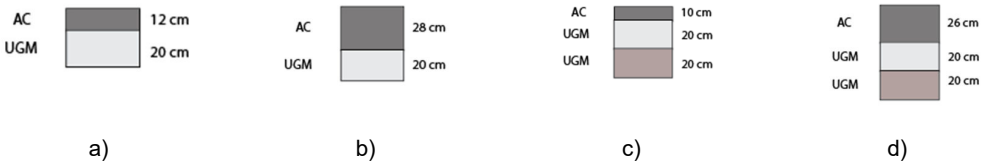

a) b) c) d)

AC – asphalt concrete; UGM – unbound granular material

Figure 4.4 - Flexible pavements from MACOPAV manual, F3 foundation

a) b) c) d)

AC – asphalt concrete; UGM – unbound granular material

Figure 4.5 –Flexible pavements from MACOPAV manual, F2 foundation

Two types of flexible pavements were chosen, one is asphalt bound base (a, b) and the other is unbound aggregate base. (c, d). The force load simulated were 65 kN and 90 kN. Once the deflection basins were calculated, the critical values were obtained from equation 4.2 (flexible pavement, N=3 for maximum uncertainty analysis) were used to calculate the critical value intervals as expressed in equation 4.6. The interval of deflection values represents the uncertainty present in any FWD test performed. A range of upper and lower limit values of deflection then is obtained, with wider range of values symbolizing higher uncertainty levels and, in the opposite case, a lower uncertainty, thus higher precision amongst the FWD fleet.

$$U = D \pm \mathrm{z} \tag{4.6}$$

The interval of deflection, with both higher and lower limits, constituted the basis for the sensitivity analysis. These boundaries were each backcalculated to obtain their respective elastic moduli. In other words, with the basic MACOPAV pavement models, the uncertainty interval of deflections was calculated beginning with layer material's reference moduli, and through backcalculation it was possible to obtain their equivalent layer moduli for each pavement model.

Figure 4.6, Figure 4.7, Figure 4.8 and Figure 4.9 present deflection charts with backcalculated curves superimposed to their respective limits. It represents the quality of adjustment of the backcalculation process, obtaining from that a range of maximum (stiffer) and minimum (softer) moduli for each layer.

The adjustment of the backcalculated curves in relation to the uncertainty boundary was satisfactory. The RMS error achieved in each iterative process was below 4%. This fact was well expected as the pavement models were well defined and the seed moduli were fitting, in contrast with the real-world scenario, where the pavement composition are previously unknown to the technicians thus the necessity to approximately assume an acceptable model through near site coring or by finding original project archives. In these cases, obtaining exact pavement models to

backcalculate is more complicated as the literature review has shown and, consequently, RMSE may be higher which may in turn indicate incorrect assumed model is being used. Chapter 4.4 may represent one of these cases.

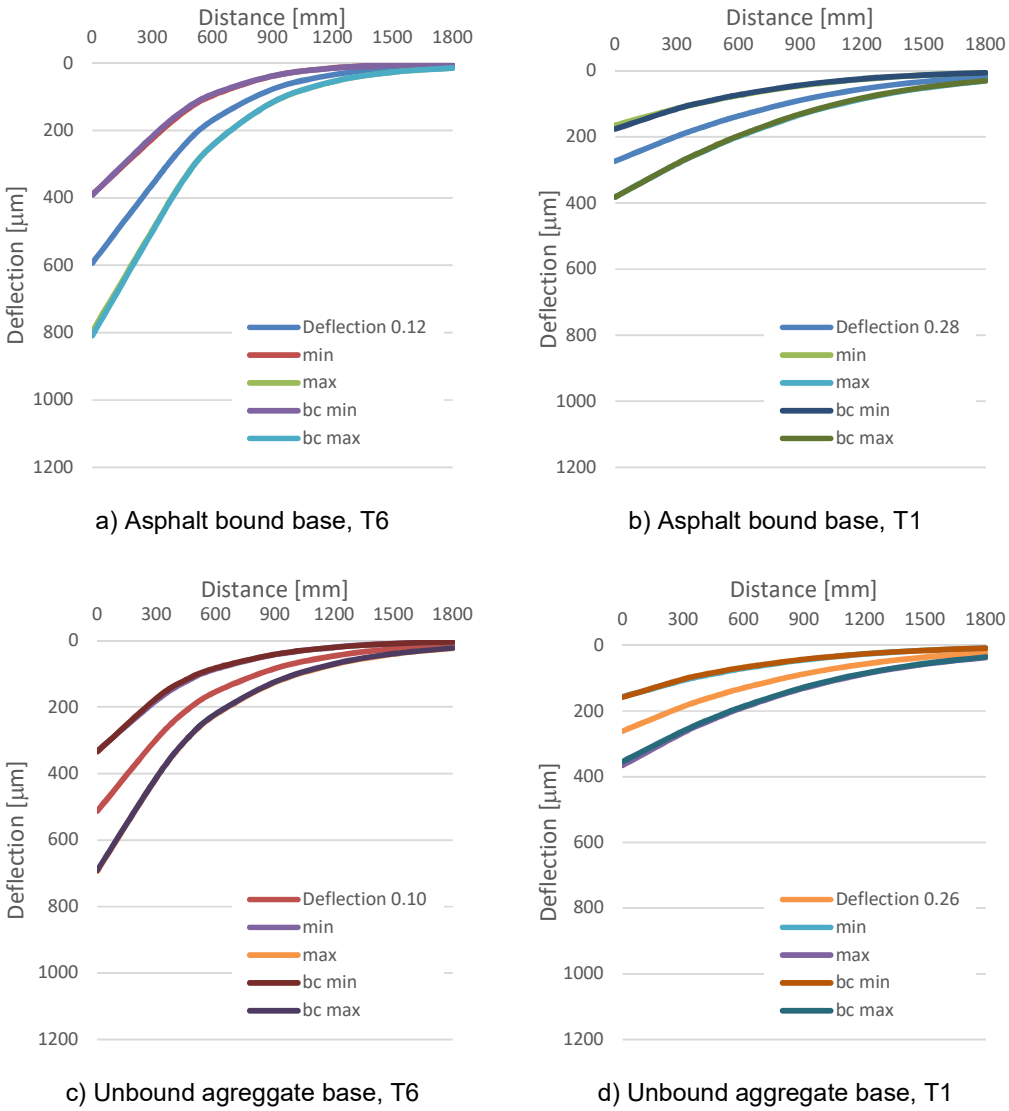

a) Asphalt bound base, T6

b) Asphalt bound base, T1

c) Unbound agreggate base, T6

d) Unbound aggregate base, T1

Figure 4.6 – Deflection charts with backcalculated curves (F3 subgrade class, 65 kN)

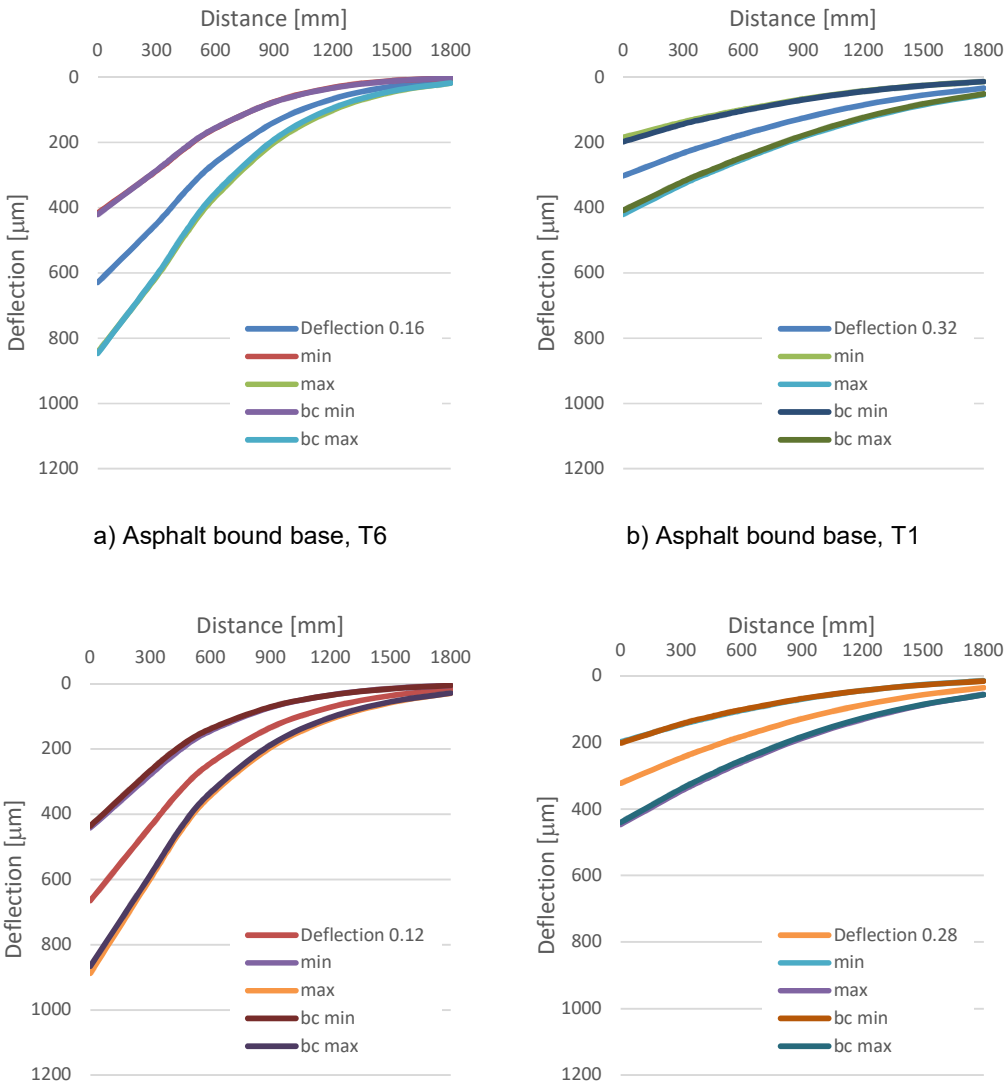

a) Asphalt bound base, T6

b) Asphalt bound base, T1

c) Unbound agreggate base, T6

d) Unbound aggregate base, T1

Figure 4.7 – Deflection charts with backcalculated curves (F2 subgrade class, 65 kN)

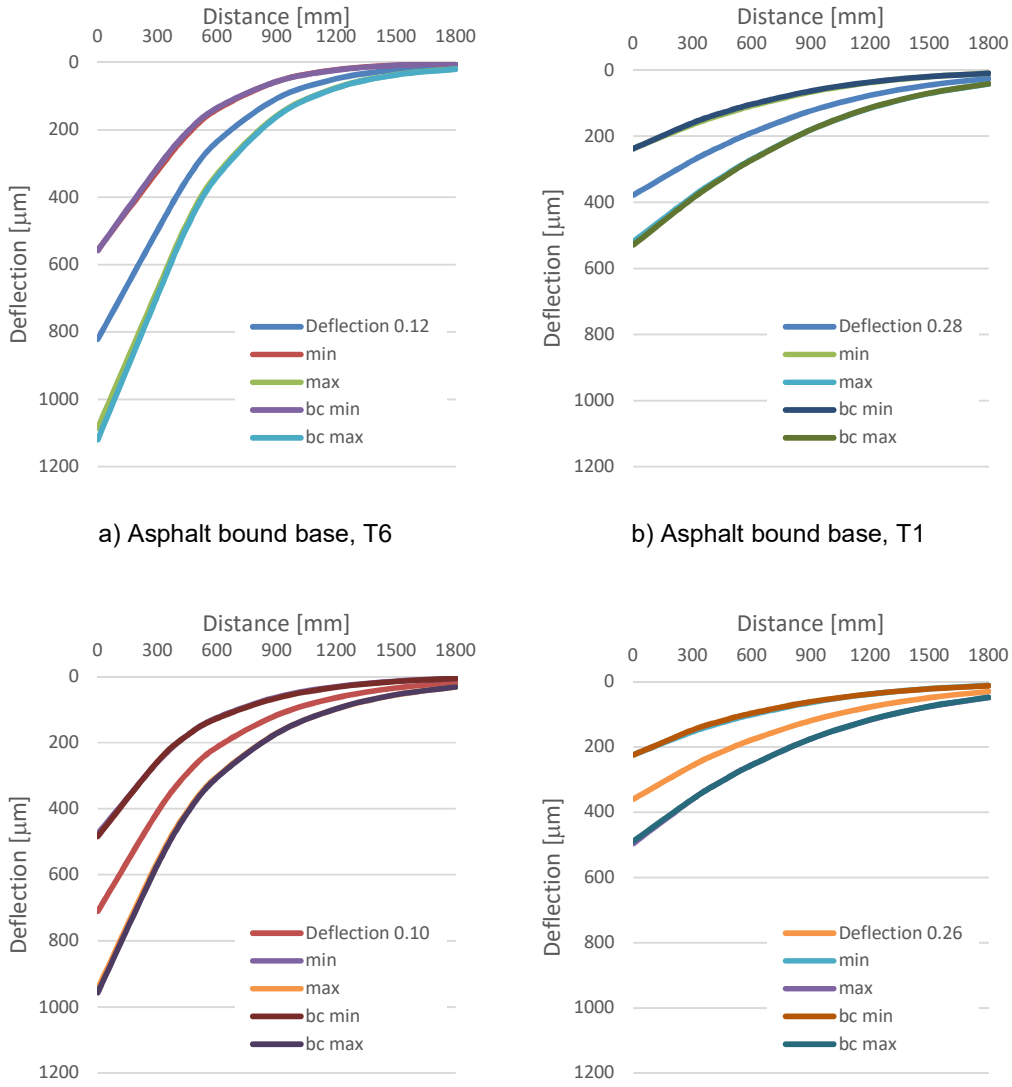

a) Asphalt bound base, T6

b) Asphalt bound base, T1

c) Unbound agreggate base, T6

d) Unbound aggregate base, T1

Figure 4.8 – Deflection charts with backcalculated curves (F3 subgrade class, 90 kN)

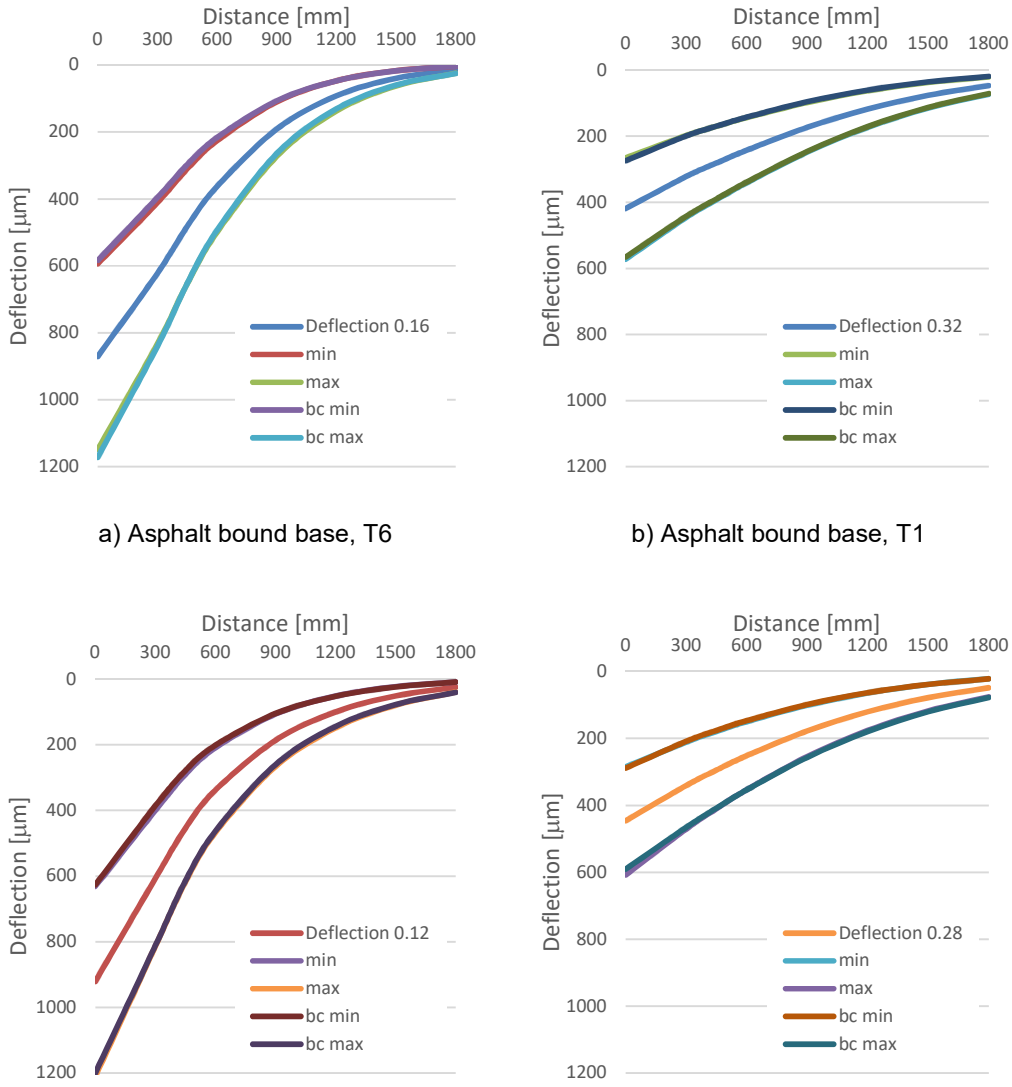

a) Asphalt bound base, T6

b) Asphalt bound base, T1

c) Unbound agreggate base, T6

d) Unbound aggregate base, T1

Figure 4.9 – Deflection charts with backcalculated curves (F2 subgrade class, 90 kN)

Table 4.2 and Table 4.3 resumes part of the backcalculated elastic moduli for the class F3 subgrade pavements subjected to 65 kN and 90 kN surface loads (see Appendix VII for all tables). It shows in a clear manner that the MACOPAV models presented convergent estimation of layer moduli for either 65 kN or 90 kN. In this way, the FWD fleet measurement uncertainty is now represented in the form of layer moduli, with the higher and the lower limits of the interval. In this form, it is possible to assess the range of moduli uncertainty when performing field surveys and even evaluate financially the same uncertainty although this study is outside the scope of the present dissertation.

Table 4.2 – Interval of pavement layer moduli, F3 subgrade class, 65 kN and 90 kN

Asphalt bound base, T6, 65 kN		
RMS 3.6%	**Reference**	**RMS 0.9%**
E_{max} (1)	**E (2)**	**E_{min} (3)**
4700	4000	3000
300	200	160
175	100	70
Asphalt bound base, T6, 90 kN		
RMS 4.0%	**Reference**	**RMS 2.7%**
E_{max} (1)	**E (2)**	**E_{min} (3)**
4500	4000	3000
300	200	180
165	100	70

Asphalt bound base, T1, 65 kN		
RMS 3.6%	**Reference**	**RMS 2.3%**
E_{max} (1)	**E (2)**	**E_{min} (3)**
4500	4000	3000
400	200	140
200	100	70
Asphalt bound base, T1, 90 kN		
RMS 3.5%	**Reference**	**RMS 1.2%**
E_{max} (1)	**E (2)**	**E_{min} (3)**
5000	4000	3500
390	200	150
190	100	75

Units in MPa; (1) – Layer modulus for stiffer limit layer composition; (2) – Reference layer moduli; (3) – Layer modulus for softer limit layer composition.

Table 4.3 – Interval of pavement layer moduli, F3 subgrade class, 65 kN and 90 kN

Unbound aggregate base, T6, 65 kN		
RMS 2.8%	**Reference**	**RMS 1.5%**
E_{max} (1)	**E (2)**	**E_{min} (3)**
4300	4000	3300
600	400	300
330	200	150
180	100	70
Unbound aggregate base T6, 90 kN		
RMS 3.9%	**Reference**	**RMS 1.0%**
E_{max} (1)	**E (2)**	**E_{min} (3)**
4300	4000	3300
600	400	300
310	200	150
160	100	70

Unbound aggregate base T1, 65 kN		
RMS 3.6%	**Reference**	**RMS 2.5%**
E_{max} (1)	**E (2)**	**E_{min} (3)**
5000	4000	3300
750	400	290
360	200	130
200	100	70
Unbound aggregate base T1, 90 kN		
RMS 3.9%	**Reference**	**RMS 0.7%**
E_{max} (1)	**E (2)**	**E_{min} (3)**
5000	4000	3300
700	400	290
360	200	130
190	100	70

Units in MPa; (1) – Layer modulus for stiffer limit layer composition; (2) – Reference layer moduli; (3) – Layer modulus for softer limit layer composition.

Figure 4.10 presents a final visual representation of the variation of each layer moduli. The variation in moduli values necessary to adjust the initial reference moduli to the critical values boundaries are expressed in function to the asphalt concrete material content in relation to the pavement total thickness (in percentage). From top to bottom, Top layer - Base - Sub-base - Subgrade, both the granular material layer required more adjustment, reaching as high as 80%, leading to stiffer layers for pavements with higher content of asphalt concrete (more than 40%). Pavement models with higher flexibility present higher sensitivity to FWD uncertainties.

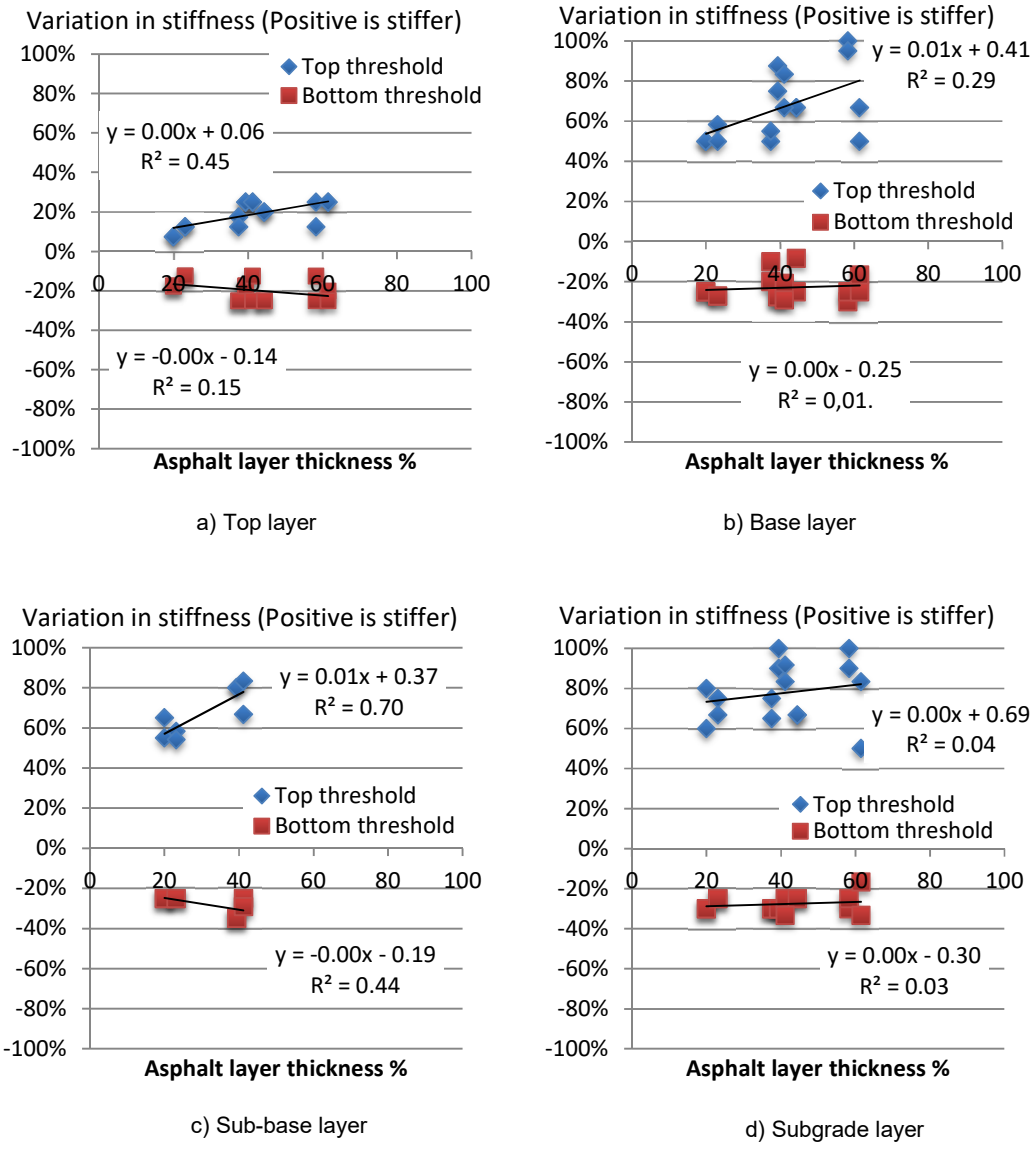

Figure 4.10 – Variation in critical stiffness values in relation to percentage of asphalt concrete layer thickness over pavement's total thickness

4.4 Test site backcalculation

Regarding test site 1, the PTS results confirmed the findings included in chapter 4.3. The backcalculation of deflection measurements resulted in three different pavement designs, each influenced by the uncertainty already mentioned. In the event of a rehabilitation project, these results could directly affect the possible project solutions, namely when determining the necessary thickness of the overlay design, poising financial impacts on the project's final cost.

Figure 4.11 and Figure 4.12 show deflection plot charts with BC deflection curve layered on top. RMSE obtained were between 6.0 to 8.4%. High RMSE values were obtained representing that the pavement model might not exactly match the actual pavement.

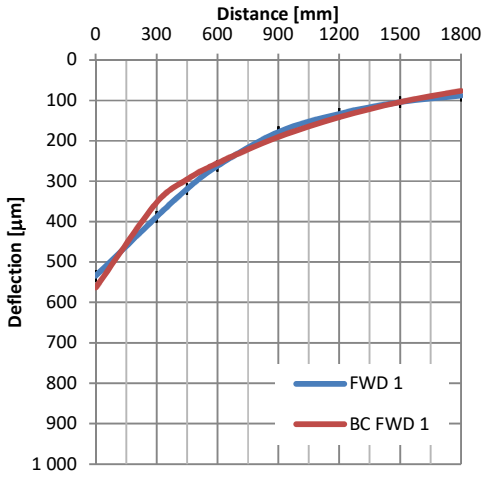

a) FWD 1

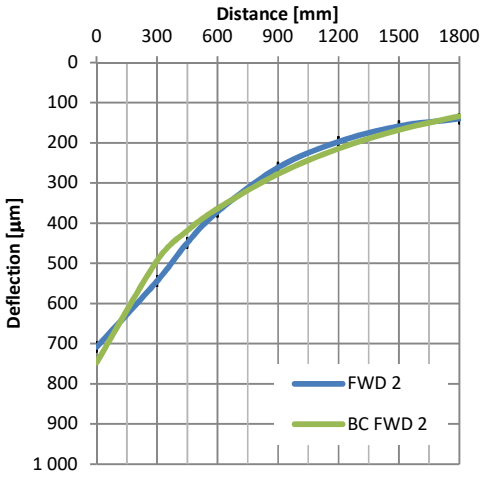

b) FWD 2

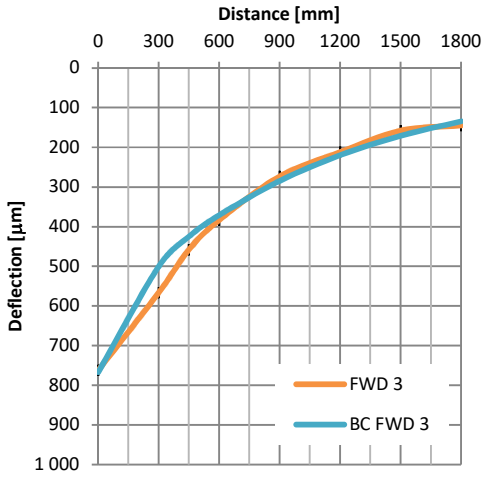

a) FWD 3

Figure 4.11 – Deflection chart with BC curve, Site 1, 65 kN

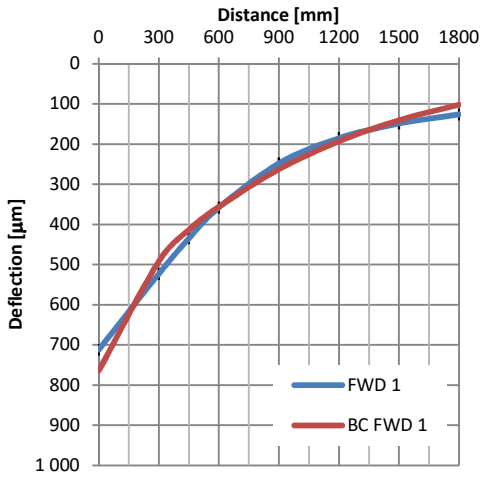

a) FWD 1

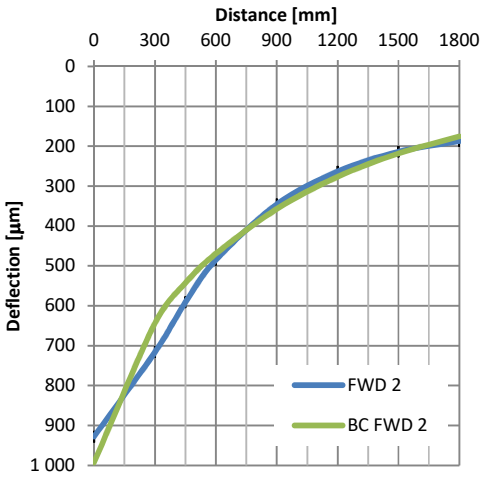

b) FWD 2

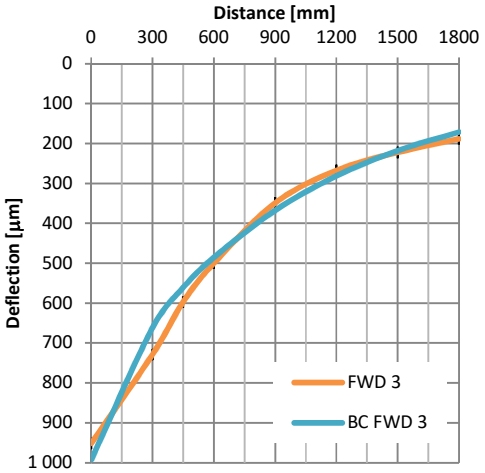

b) FWD 3

Figure 4.12 – Deflection chart with BC curve, Site 1, 90 kN

The AC top layer of just only 5 cm of thickness may also contribute to a less responsive model in BC software when adjusting such thin layer stiffness. In a different note, although test site 1 is an asphalt bound pavement, it was discovered that its asphalt content in the mix was not very significant which may modify its mechanical behavior when comparing to other proper asphalt mix pavements (see Appendix VIII).

Table 4.4 and Table 4.5 summarizes the Test Site 1 pavement model backcalculated moduli. FWD 1 clearly presents stiffer pavement estimation due to its lower deflection recordings. FWD 2 and 3 present moduli in similar value magnitude representing good reproducibility between the two, although no there are no information if both FWD tested with similar load pulse time.

In conclusion, the backcalculation of deflections measured independently by FWD 1, 2, 3 produced what can be considered an acceptable estimation of a multi-layer pavement model elastic moduli.

Table 4.4 – Backcalculation results for Site 1, 65 kN

AC – Asphalt concrete; UGM - Unbound granular material; Root Mean Square Error (%)

Layer	Material	Thickness [cm]	Seed moduli	FWD 1	FWD 2	FWD 3
Surface	AC	5	4000	9500	6000	7000
Base	UGM	20	900	600	600	500
Sub-base	Soil-cement	15	900	1200	600	900
	Sandy soil	15	50	200	90	75
	Sandy soil	100	30	40	50	40
RMS%				7.4	6.5	6.6

Table 4.5 – Backcalculation results for Site 1, 90 kN

Layer	Material	Thickness [cm]	Seed moduli	FWD 1	FWD 2	FWD 3
Surface	AC	5	4000	9000	6000	6500
Base	UGM	20	900	700	600	650
Sub-base	Soil-cement	15	900	1200	600	600
	Sandy soil	15	50	80	90	80
	Sandy soil	100	30	45	60	50
RMS%				8.4	6.2	6.0

AC – Asphalt concrete; UGM - Unbound granular material; Root Mean Square Error (%)

4.5 Summary

Repeatability analysis for deflection measurement resulted in acceptable repeatability limits. In contrast, reproducibility analysis showed that the tested FWD could not reproduce each other's deflection results within a reasonable reproducibility limit. Consequently, the sensitivity analysis for 95% confidence level were conducted with high standard deviation values which, in turn, resulted in wide critical value intervals. The interval of deflection values represents the range of upper and lower limit values of a random test performed by any given FWD in the fleet.

Standardized pavement models from MACOPAV (JAE, 1995) were used as reference base for the sensitivity analysis of backcalculated moduli. With standardized pavement models layer moduli backcalculated for both higher and lower stiffness uncertainty intervals, an analysis of the variation of each layer moduli from initial reference values in relation to asphalt concrete material in the pavement total thickness in percentage was performed to find which layer presented higher uncertainty under the backcalculation process. From top to bottom (Top layer - Base - Sub-base - Subgrade), both the granular material layer required more adjustments, as high as 80%, leading to estimated stiffer layers for pavements with higher content of asphalt concrete (more than 40%). Pavement models with higher AC percentage present higher sensitivity to FWD uncertainty. These BC estimated moduli RMSE were successfully kept under 4%. It also showed that the MACOPAV models presented a convergent estimation of layer moduli for either 65 kN or 90 kN. In this way, the FWD fleet measurement uncertainty is represented in the form of layer moduli, the higher and the lower limits of the interval, enabling a direct assessment of the range of moduli uncertainty when performing field surveys and even evaluating the financial implications although this study resides outside the scope of the present dissertation.

The sensibility analysis performed in this section portrays some of the uncontrollable and the randomly unknown factors that may influence the outcome of this study. There for it is crucial to be conservative while conducting these assessments.

5 Conclusion and recommendations

5.1 Summary

Pioneering campaigns such as the WASHO (1952-1954) (WASHO, 1954) and AASHO Road Test (1963) (AASHO, 1962) marked the beginning of the development of pavement engineering and also marked the beginning of the development of equipment for performing pavement tests. Prior to the 1930's, road maintenance responsibility was attributed to the local authorities. Based on the literature review, road maintenance is viewed as being less favored than road design and construction. The focus shift from road maintenance to asset management (Madelin, 2000) motivated the development of testing methods capable of increasing network level campaigns efficiency. Non-destructive tests (NDT) became widely accepted as it enabled maintenance without resulting in road service disruption and avoided exposing workers to danger. Measuring deflections constitutes the simplest approach to evaluate qualitative parameters such as the bearing capacity of the sample. By applying a known force to the testing sample, we can measure how much it yields. To complete the characterization, physical properties can be determined by backcalculating deflection measurements, thus obtaining the wanted elastic moduli.

The objective of the present dissertation is to study the precision and uncertainty performance in FWD testing. This static impulse generating deflectometer is currently used as the standard deflection testing equipment (ASTM, 2009), mainly in point-to-point, project level, pavement testing campaigns. The FWD can measure the complete deflection bowl necessary to back calculate the multiple pavement layers underneath. The force pulse generated can simulate the action of a rolling wheel axel on the pavement. It is also significantly more mobile and easier to operate.

An experimental research in form of a proficiency test scheme (PTS), compliant with ISO/IEC 17043, organized under RELACRE, a fleet of three FWD were tested. An assessment of repeatability and reproducibility performance was performed. An uncertainty analysis followed allowing a better understanding of uncertainty's influence to the quality of pavement structural capacity assessments, for example, in case of a structural quality evaluation to support a rehabilitation project. Lastly, a sensitivity analysis with standardized MACOPAV pavement models was also produced.

The experimental research results confirmed a satisfactory repeatability of deflection measurements. In contrast, the reproducibility is difficult to achieve in most cases. Consequently, the uncertainty levels revealed to be high. Uncertainty and precision revealed to be dependent of pavement type and deflection magnitude. Uncertainty presented high values for flexible pavement and for high deflections. Regarding to the sensitivity analysis on the uncertainty's influence on the FWD results interpretation, it was concluded that the flexible pavements presented higher sensibility to uncertainty mainly when gauging for stiffness on the foundation layers.

5.2 Conclusions

The current dissertation allowed to find and aggregate several conclusions. Road and airfield pavement management is getting increasing attention in the engineering and business management fields as an opportunity to develop more technologically advanced and efficient methodologies to assess pavement condition at a network level, while enhancing the performance of the asset management in a competitive business sector. The practice has evolved from early XX century static or slow deflectometers to current developing traffic speed deflectometers, with

mobile computerized pavement condition assessment and data transfer to existing pavement management system.

The most used deflection measurement device is the FWD. The FWD is widely adopted by most road and airfield administrations to conduct routine pavement tests. Its popularity has promoted the existence of numerous peer reviewed articles and active regional user groups. In this scope, the proposed dissertation developed an experimental research featuring three FWD from different manufacturers (Dynatest, Carl Bro and KUAB). A proficiency test scheme developed to retrieve data from the FWD fleet to assess uncertainty's influence on test results. The main conclusions were:

- Repeatability and reproducibility limits result were dependent of deflection magnitude as well as pavement stiffness.
- Repeatability limit for the flexible pavements test site was r=4 and for the rigid pavement test site r=2.
- Reproducibility limits were higher and in function of any given deflection value. The trend line presented a steep slope, which towards the higher range of deflection presented the maximum reproducibility limit. For an assumed deflection of D_f=300 nm, flexible pavement test site limit value was R=169 and for the rigid pavement test site, the limit value was R=93.

These results are in line with the reviewed literature (Garg, 2002; Murphy, 1998; Rocha et al, 2004) that thoroughly studies FWD repeatability and reproducibility. Although repeatability is normally achieved, reproducibility is dependent of ambient factors and each FWD feature, such as the deflectometer types, the analog-to-digital signal interpretation algorithm proprietary of each manufacturer, the quality of the rubber on the bottom of the loading plate, the shape and quality of the rubber buffers, the load pulse history, the drop height, the force frequency, and many other variables that make reproducibility hard to control effectively.

The accuracy of the pavement model determined for moduli backcalculation process play an important role in the success outcome of the analysis. Literature review indicate that loosely defined models produce high RMSE values which in turn poses difficulties to achieve correctly estimated layer moduli (Irwin, 2002). Reproducing pavement models exact to real location is difficult due to heterogeneity of layer properties and parameters in both in depth and longitudinally.

The backcalculation analysis performed under FWD uncertainty resulted in a range of interval for estimated moduli, representing the type of varying results that may be obtained attending to the reproducibility issues reported by literature. Backcalculation methods are not 100% straightforward and depends on several input parameters, such as the seed moduli, layer thickness, temperature, the pavement model, etc. The exercise of backcalculating MACOPAV pavement models produced a study of measured deflections that were backcalculated to layer moduli for two peak nominal loads, 65 and 90 kN. The result was a converging set of pavement layer moduli interval. These results can also, in turn, be used to evaluate uncertainty's influence in proposed rehabilitation designs and the corresponded financial implications. The main conclusions were:

- The adjustment of the backcalculated curves in relation to the uncertainty boundary was satisfactory. The RMS error achieved in each iterative process was below 4%.

- The variation in moduli values necessary to adjust the initial reference moduli to the critical values boundaries were expressed in function to the asphalt concrete thickness in relation to the pavement total thickness (in percentage) and several conclusions were found:
    - Granular layers required more adjustment, reaching as high as 80%, leading to stiffer layers for pavements with higher flexibility (more than 40%). Foundation layers also required more adjustment, around 80%, when adjusted to the uncertainty curves.
    - Backcalculated moduli sensitivity to FWD uncertainties are directly linked to the pavement's flexibility, i.e., highly flexible pavements are affected with higher uncertainty's influence.

In conclusion, the initial objectives of the dissertation were accomplished. A repeatability and reproducibility analysis were successfully completed with data measured on site. This analysis was followed in an uncertainty assessment, which revealed that uncertainty was dependent of deflection values magnitude and pavement stiffness itself. Finally, the sensitivity analysis concluded that the more flexible the pavements presented the tendency to be more sensitive to FWD uncertainty.

5.3 Recommendations

As a final remark of this study several recommendations are suggested.

Both the literature review and the field trial provided evidence that FWD performance is bound to be influenced by random sources of uncertainty. To attain a satisfactory level of confidence, FWD operators should have a thorough understanding of the FWD functionalities and its operation principles. Environmental interferences such as the temperature's effect on the pavement surface and the buffer system play some part in the accuracy variation. In addition, the interpretation of load time history (if allowed by the FWD model) and the acknowledgement of the high frequency cut off function are all requirements to provide a valid interlaboratory comparison and thus a better quality assessment in pavement engineering.

FWD operators should always be entitled to continuous training achieving better theoretical knowledge underlying routine operations.

The scope of this study did not contemplate the financial burden of poorly performed FWD analysis, such as backcalculating high uncertainty deflection measurements resulting in misleading pavement models subjected to rehabilitation project design. The author wishes to suggest this exercise from another opportunity of study which would be interesting and insightful. This opportunity would provide pavement engineers and decision makers with a sense of reality of the financial cost that could exist when calling for tender for new projects.

References

AASHO (1962). “The AASHO The road test”. American Association of State Highway and Transportation Officials, Washington, USA.

Alkasawneh, W. (2007). “Backcalculation of pavement moduli using genetic algorithms”. *PhD dissertation.* University of Akron. Ohio, USA.

Andersen, S., Levenberg, E., & Andersen, M. B. (2017). “Inferring pavement layer properties from a moving measurement platform”. *BCRRA 2017 - 10th International Conference on the Bearing Capacity of Roads, Railways and Airfields. Athens, Greece.*

Andrén, P. (2006). “Development and Results of the Swedish Road Deflection Tester”. Retrieved from http://www.diva-portal.org/smash/get/diva2:10556/FULLTEXT01.pdf. (Date Accessed: August 25, 2016)

Antonsen, V., & Mork, H. (2017). “A comparison of TSD and FWD deflections at Norwegian roads with an interpretation of bearing capacity from TSD measurements”. *BCRRA 2017 - 10th International Conference on the Bearing Capacity of Roads, Railways and Airfields. Athens, Greece.*

Antunes, M. L. (1997). “Desenvolvimento de modelos de degradação de pavimentos”. *Colóquio sobre Conservação, Junta Autónoma de Estradas. Lisbon*, Portugal

ASTM (1999). ASTM D6433-99 “Standard Practice for Roads and Parking Lots Pavement Condition Index Surveys”. ASTM International.

ASTM (2008). ASTM D4695–03 “Standard Guide for General Pavement Deflection Measurements”. ASTM International.

ASTM (2009). ASTM D4694-09 “Standard Test Method for Deflections with a Falling-Weight-Type Impulse Load”. *ASTM International*.

AUSTROADS (2006). “Guide to Asset Management Part 5E: Cracking”. Retrieved from https://www.onlinepublications.austroads.com.au/items/AGAM05E-06. (Date accessed: July 26, 2017).

AUSTROADS (2007a). “Guide to Asset Management Part 5B: Roughness”. Retrieved from https://www.onlinepublications.austroads.com.au/items/AGAM05B-07. (Date accessed: July 26, 2017).

AUSTROADS (2007b). “Guide to Asset Management Part 5C: Rutting”. https://www.onlinepublications.austroads.com.au/items/AGAM05C-07. (Date accessed: July 26, 2017).

AUSTROADS (2008). “Guide to Asset Management Part 5D: Strength”. Retrieved from https://www.onlinepublications.austroads.com.au/items/AGAM05D-08. (Date accessed: July 26, 2017).

AUSTROADS (2009a). “Guide to Asset Management Part 5F: Skid Resistance”. Retrieved from https://www.onlinepublications.austroads.com.au/items/AGAM05F-09. (Date accessed: July 26, 2017).

AUSTROADS (2009b). “Guide to Asset Management Part 5G: Texture”. Retrieved from https://www.onlinepublications.austroads.com.au/items/AGAM05G-09. (Date accessed: July 26, 2017).

AUSTROADS (2009c). “Guide to Pavement Technology Part 7: Pavement Maintenance”. Retrieved from https://www.onlinepublications.austroads.com.au/items/AGAM05C-07. (Date accessed: July 26, 2017).

AUSTROADS (2011). “Guide to Pavement Technology Part 5: Pavement Evaluation and Treatment Design”. Retrieved from https://www.onlinepublications.austroads.com.au/items/AGPT05-11. (Date accessed: July 26, 2017).

Benbow, E., & Wright, A. (2012). “HERoad (Holistic Evaluation of Road Assessment) Deliverable 1.1 – Pavement performance assessment”. Retrieved from http://vti.diva-portal.org/smash/get/diva2:814340/FULLTEXT01.pdf.

Bentsen, Nazarian, S., & Harrison. (1989). “Reliability Testing of Seven Nondestructive Pavement Testing Devices”. Nondestructive Testing of Pavements and Backcalculation of Moduli, STP 1026, pp. 41-58. *American Society of Testing and Materials, Philadelphia, USA*.

Bohn, A. O. (1989). “The History of the Falling Weight Deflectometer”. Retrieved from http://www.pavement-consultants.com/media/6042/HistoryOfFWD_AxelOBohn.pdf (Date accessed: August 9, 2016)

Branco, F., Pereira, P., & Picado Santos, L. (2008). “Pavimentos Rodoviários”. Edições Almedina. Coimbra, Portugal.

Brown, S. F., & Pappin, J. W. (1981). “Analysis of pavements with granular bases”. *Transportation Research Record, 810, pp. 17-23*.

Bush, J. A., & Baladi, G. Y. (1989). “Nondestructive testing of pavements and backcalculation of moduli”. International Symposium on Nondestructive Testing of Pavements and Backcalculation of Moduli, 1st, 1988, Baltimore, Maryland, USA.

Chen, D., Bilyeu, J., He, R., & Murphy, M. (1999). “Effects of Buffers on Falling Weight Deflectometer Measurements”. Internal Technical Memo, Design Pavement Section, TxDOT. Austin, Texas.

Choubane, B., Gokhale, S., Mike Jackson, N., & Nazef, A. (2006). “Assessing the Precision of Falling Weight Deflectometer for Field Measurements”. J*ournal of ASTM International*, Vol. 3, No. 3, 2006, pp. 1-12.

Čičković, M. (2017). “Analysing FWD data — from the deflection bowl to material parameters”. *BCRRA 2017 - 10th International Conference on the Bearing Capacity of Roads, Railways and Airfields. Athens, Greece.*

Claessen, A., Edwards, J., Sommer, P., & Ugé, P. (1977). “Asphalt Pavement Design Manual: The SHELL Method”. University of Michigan. Michigan, USA.

Clarke, D. B., Harris, S. B., Heitzman, A. C., & Margiotta, R. A. (2003). “SHRP Long-Term Pavement Performance Information Management System”. Transportation Research Record 1260.

Correia, J. M. S. (2014). “Retro-análise de Resultados de Caracterização Estrutural de Pavimentos”. Dissertação de mestrado. Instituto Superior Técnico.

COST (1997). “COST 325 - New Road Monitoring Equipment and Methods. Final Report of the Action”. Directorate General Transport. European Comission.

COST (1998). “COST 336 – Information Gathering Report, Task Group 2 - FWD at Network Level”. Final draft report. European Comission.

Dormon, G. M. & Metcalf, C. T. (1965). “Design curves for flexible pavements based on layered system theory”. *43rd Annual Meeting of the Committee on Flexible Pavement Design*.

Estradas de Portugal (1995). “Manual de Dimensionamento do Reforço de Pavimentos Flexíveis”. Estradas de Portugal.

European Commission. (2005). “FORMAT, Fully Optimised Road Maintenance, Final Technical Report”. European Commission.

Eurostat (n.d.-a). “Freight transport statistics - modal split”. Retrieved from http://ec.europa.eu/eurostat/statistics-explained/index.php/Freight_transport_statistics_-_modal_split. (Date accessed: April 8, 2017).

Eurostat (n.d.-b). “Trans-European networks in transport (TEN-T)”. Retrieved from http://ec.europa.eu/eurostat/statistics-explained/index.php/Trans-European_networks_in_transport_(TEN-T) . (Date accessed: April 8, 2017).

Fernando, E., Liu, W., & Ryu, D. (2001). “Development of a procedure for temperature correction of backcalculated AC modulus”. Texas: Texas Transportation Institute.

Fileccia Scimemi, G., Turetta, T., & Celauro, C. (2016). Backcalculation of airport pavement moduli and thickness using the Levy Ant Colony Optimization Algorithm. *Construction and Building Materials, Vol. 119, pp. 288-295*.

Flores, J. M., Van, P. Le, Park, C. K., Kim, W., & Lee, H. J. (2017). “Development of a frequency temperature correction model for FWD back-calculated moduli based on frequency-temperature superposition principle”. *BCRRA 2017 - 10th International Conference on the Bearing Capacity of Roads, Railways and Airfields. Athens, Greece.*

Fontul, S. (2004). “Strutural Evaluation of Flexible Pavements Using Non-Destrutive Tests”. Tese de Doutoramento. Departamento de Engenharia Civil. Universidade de Coimbra.

Francisco, A. (2012). “Comportamento estrutural de pavimentos rodoviários flexíveis”. Dissertação de Mestrado. Instituto Politécnico de Bragança.

Fwa, T., Chan, W., & Hoque, K. (2000). “Multiobjective optimization for pavement maintenance programming”. *Journal of Transportation Engineering, 126 (5), pp. 367-374*.

Garbowski, T., & Pożarycki, A. (2016). “Multi-level backcalculation algorithm for robust determination of pavement layers parameters”. *Inverse Problems in Science and Engineering*, Vol. 25 (5), pp. 674-693.

Garg, N. (2002). “Comparison between falling weight deflectometer and static deflection measurements on flexible pavements at the national airport pavement test facility (NAPTF)”. Federal Aviation Administration. Retrieved from airtech.tc.faa.gov/Pavement/Downloads/P-15.pdf. (Date accessed: April 24, 2017)

Goldberg, D. E. (1989). “Genetic Algorithms in Search, Optimization, and Machine Learning”. Addison-Wesley Professional. Reading, Massachusetts, USA.

Irwin, L. H. (2002). “Backcalculation : An Overview and Perspective”. *FWD Backcalculation Workshop 3 – 6th International Conference on the Bearing Capacity of Roads, Railways and Airfields - BCRA 2002*.

ISO (1994a). ISO 5725-1-1994 Accuracy (truness and precision) of measurement methods and results. International Organization of Standarization.

ISO (1994b). ISO 5725-2-1994 Accuracy (truness and precision) of measurement methods and results. International Organization of Standarization.

ISO (2010). ISO 17043-2010 Conformity assessment - General requirements for proficiency testing. International Organization of Standarization.

JAE (1995). “MACOPAV - Manual de Concepção e Pavimentos para a Rede Rodoviária Nacional”. Portugal.

JAE (1997). Catálogo de Degradações dos Pavimentos Rodoviários Flexíveis. Junta Autónoma de Estradas. Portugal.

Johnson, A. M. (2000). “Best Practice Handbook on Asphalt Pavement Maintenance”. Center for Transportation Studies, University of Minnesota. Minnesota, USA.

Leiva-Villacorta, F. (2012). “Determination of Correction Factors for the High Frequency / High Speed FWD Pavement Responses to Typical Operating Speed Responses”. Retrieved from http://www.asphalttechnology.org/downloads/(13)-AAPT-2012-Villacort.pdf. (Date accessed: August 4, 2017).

Lukanen, E. O. (1992). “Effects of buffers on falling weight deflectometer loadings and deflections”. *Transportation Research Record, No. 1355, pp. 37-51*.

Madelin, K. B. (2000). “Developments in Maintenance Management in the United Kingdom”. *International Journal of Pavement Engineering, Vol. 1 (3), pp. 233-245*.

Madsen, S. S., & Levenberg, E. (2017). “Dynamic backcalculation with different load-time histories”. *Road Materials and Pavement Design, pp. 1-20*. Taylor & Francis. https://doi.org/10.1080/14680629.2017.1307263

Meneses, S., & Ferreira, A. (2012). “Pavement maintenance programming considering two objectives: maintenance costs and user costs”. *International Journal of Pavement Engineering*. https://doi.org/10.1080/10298436.2012.727994

Murphy, M. (1998). “A Mechanistic-Empirical Approach to Characterizing Subgrade Support and Pavement Structural Condition for Network-level Application”. PhD dissertation. University of Texas, Austin, USA.

NPMA (1999). “Pavement Surface Condition Field Rating Manual for Asphalt Pavements”. Northwest Pavement Management Association.

Oshone, M., Elshaer, M., Dave, E., & Daniel, J. S. (2017). “Evolution of asphalt modulus from falling weight deflectometer tests and challenges associated with its interpretation and applications: A case study using LTPP data”. *BCRRA 2017 - 10th International Conference on the Bearing Capacity of Roads, Railways and Airfields. Athens, Greece.*

Pais, J. C., & Pereira, P. (2017). “A model to adjust the falling weight deflections due to temperature variations”. *BCRRA 2017 - 10th International Conference on the Bearing Capacity of Roads, Railways and Airfields. Athens, Greece.*

Picado-Santos, L., Ferreira, A., & Pereira, P. (2006). “Estruturação de um sistema de Gestão de Pavimentos para uma Rede Rodoviária Nacional”. *Revista Engenharia Civil, Universidade Do Minho, Nº 26*.

Quintus, H., Bush, A., & Baladi, G. (1994). “Nondestructive testing of pavements and backcalculation of moduli”. ASTM special technical publications. Phladelphia, PA. USA.

Rakesh, N., Jain, A. ., Reddy, M. A., & Reddy, K. S. (2006). “Artificial neural networks—genetic algorithm based model for backcalculation of pavement layer moduli”. *International Journal of Pavement Engineering*. https://doi.org/10.1080/10298430500495113

Rocha, S., Tandon, V., & Nazarian, S. (2001). “Reproducibility of Texas Department of Transportation Falling Weight Deflectometer Fleet”. Center for Highway Materials Research. University of Texas.

Rocha, S., Tandon, V., & Nazarian, S. (2004). “Falling Weight Deflectometer Fleet: Repeatability and Reproducibility”. *Road Materials and Pavement Design, Vol. 5 (2), pp. 215-238.*

Rohde, G. T., & Scullion, T. (1990). “MODULUS 4.0: Expansion and Validation of the MODULUS Backcalculation System”. Texas Transportation Institute, Texas A&M University System, College Station.

Salt, G., & Stevens, D. (2007). “Modular ratios for unbound granular pavement layers”. *Tonkin and Taylor Ltd, Dunedin, New Zealand*.

Santinho Horta, C., Costa Pereira, F., Lopes, S., & Morgado, J. (2011). “O Sistema de Gestão de Conservação de Pavimentos da Implementação Consolidada - Balanço de uma

Implementação Consolidada". *7º Congresso Rodoviário Português*. Lisboa, Portugal.

Shell (1995). "BISAR - User Manual". Bitumen Business Group.

Sorensen, A. (1993). "Dynatest FWD/HWD field programs - smoothed (signal) peak option". (Laboratorire Central des Points et Chaussées, Ed.), *2nd FWD Seminar of Forum of European National Highway Research Laboratories (FEHRL)*. Bouguenais: Laboratorire Central des Points et Chaussées.

Steer Davies Gleave. (2009). "Ex Post Evaluation of Cohesion Policy Programmes 2000-2006 Work Package 5A : Transport. First Intermediate Report".

Tayabji, S., & Lukanen, E. O. (2000). "Nondestructive testing of pavements and backcalculation of moduli, Third Volume". ASTM special technical publication. West Conshohocken, PA.

Van Gurp, C. (1991). "Consistency and Reproducibility of Falling Weight Deflections". *Road and Airport Pavement Response Monitoring Systems-Conference Proceedings*, pp. 291-305. West Lebanon, New Hampshire, USA.

Van Gurp, C. (1995). "Characterization of seasonal influences on asphalt pavements with the use of falling weight deflectometers". PhD dissertation. Technische Universiteit Delft.

WASHO (1954). "The WASHO Road Test". National Research Council (U.S.). Highway Research Board.

Wright, A., Benbow, E., Spielhofer, R., Sjögren, L., Hildebrand, G., Kokot, D., Rabe, R. (2016). "Hi-SPEQ – Developing the Technical and Quality Requirements for High-speed Condition Surveys of Road Networks". *Transportation Research Procedia*. https://doi.org/http://dx.doi.org/10.1016/j.trpro.2016.05.417

Zofka, A., Sudyka, J., & Sybilski, D. (2017). "Assessment of pavement structures at traffic speed". *BCRRA 2017 - 10th International Conference on the Bearing Capacity of Roads, Railways and Airfields. Athens, Greece.*

Appendix

Appendix I. Proficiency test protocol

Ensaio de aptidão – 2016

Ensaio de carga com defletómetro de impacto (FWD)

Local dos ensaios:
Depósito Geral de Material da Força Aérea
Rua dos Pioneiros da Aviação
2615 – Alverca

Dia e hora:
6 de dezembro 2016 pelas 9:30

Informação a disponibilizar de cada entidade participante:

- Nome dos técnicos presentes (portaria)
- Matrícula da viatura (portaria)
- Documento de identificação (portaria)
- Comprovativo mais recente de calibração FWD (opcional)
- Gama de tolerância dos geofones do respetivo aparelho (ou apresentar os dados técnicos completos)
- Ano de fabrico/compra do equipamento (para aferir a sua geração)

Condições técnicas de realização dos ensaios:

1. Verificar as posições dos geofones
2. Verificar o diâmetro da placa de impacto
3. Medir a temperatura do ar e da superfície
4. Anotar os valores Load-pulse (sempre que possível) de cada ensaio de carga

Condições de realização dos ensaios:

- Marcação do local onde assenta a placa de impacto e a orientação da régua com os geofones.
- Diâmetro da placa de impacto: 30 cm
- Posicionamento dos geofones:

	D0	D1	D2	D3	D4	D5	D6	D7
D [mm]	0	300	450	600	900	1200	1500	1800

Tipo de pavimento	Cargas a aplicar [kN]	Número de repetições (registar todas)
Pavimento betuminoso	65, 90	2x (assentamento), 3x (repetibilidade)
Pavimento rígido	65, 90	2x (assentamento), 3x (repetibilidade)

Guia de procedimento:

Para cada entidade FWD e para cada amostra de pavimento:

1. Medição da temperatura no ar e no pavimento
2. Efetuar ensaio de carga:
    i. 2x Pré-ensaios de carga para garantir o correto contacto da placa de impacto;
    ii. 3x Ensaios de carga com captação da carga máxima gerada e dos valores das deflexões medidas. Registar dados carga-deflexão para calculo de Load-pulse quando possível.

Lisboa, 29 de outubro de 2016

Appendix I. FWD results

Table. I.1 - Site 1, 65 kN

				Distance [mm] (Deflection [μm])								
			Load [kN]	PT	0	300	450	600	900	1200	1500	1800
	FWD 1	1	65	24	534	388	319	262	178	133	104	88
		2	65	24	533	387	318	261	178	132	104	88
T_S	19	3	65	24	533	388	319	261	178	132	104	88
T_A	22	A			533	388	319	261	178	132	104	88
	FWD 2	1	65	(*)	707	544	448	371	262	198	160	140
		2	65	(*)	711	545	450	372	262	198	158	140
T_S	20	3	65	(*)	707	544	449	371	260	196	157	140
T_A	21	A			708	544	449	371	261	197	158	140
	FWD 3	1	65	24	764	572	462	383	268	203	164	142
		2	65	24	764	566	459	385	276	217	156	147
T_S	18	3	65	24	760	562	453	383	276	217	154	146
T_A	20	A			763	567	458	383	273	212	158	145

T_S – Surface temperature [°C], T_A – Air temperature [°C], PT – Pulse time [ms],
(*) – Not available

Table. I.2 - Site 1, 90 kN

				Distance [mm] (Deflection [μm])								
			Load [kN]	PT	0	300	450	600	900	1200	1500	1800
	FWD 1	1	90	24	712	523	435	358	248	185	149	126
		2	90	24	706	519	430	354	245	184	148	126
T_S	18	3	90	24	711	522	435	356	248	186	150	127
T_A	20	A			710	521	433	356	247	185	149	126
	FWD 2	1	90	(*)	928	715	591	485	347	264	213	188
		2	90	(*)	927	715	590	485	346	263	213	187
T_S	20	3	90	(*)	929	718	593	486	345	264	216	188
T_A	21	A			928	716	592	486	346	264	214	187
	FWD 3	1	90	23	950	727	595	499	346	265	221	189
		2	90	23	952	728	597	500	349	267	223	187
T_S	19	3	90	23	953	731	599	501	352	270	223	189
T_A	19	A			952	728	597	500	349	267	222	188

T_S – Surface temperature [°C], T_A – Air temperature [°C], PT – Pulse time [ms],
(*) – Not available

Table. I.3 - Site 2, 90 kN

				Distance [mm] (Deflection [μm])								
			Load [kN]	PT	0	300	450	600	900	1200	1500	1800
	FWD 1	1	90	22	284	249	229	209	173	141	116	94
		2	90	21	284	249	230	211	173	141	116	94
T_S	17	3	90	22	284	249	229	210	173	141	116	95
T_A	19	A			284	249	229	210	173	141	116	94
	FWD 2	1	90	(*)	331	295	269	249	203	167	138	114
		2	90	(*)	329	295	270	248	204	167	139	113
T_S	17	3	90	(*)	331	296	271	247	204	168	137	114
T_A	18	A			330	295	270	248	204	168	138	114
	FWD 3	1	90	23	351	311	288	264	216	180	150	124
		2	90	23	351	311	288	264	216	180	149	124
T_S	17	3	90	23	351	311	288	264	217	180	149	124
T_A	19	A			351	311	288	264	217	180	149	124

T_S – Surface temperature [°C], T_A – Air temperature [°C], PT – Pulse time [ms],
(*) – Not available

Appendix II. Smoothing filter test

Table. II.1 – Smoothing filter test results, Test site 1

				Distance [mm] (Deflection [μm])								
LP	**PT**	**SF**	**Load**	**0**	**300**	**450**	**600**	**900**	**1200**	**1500**	**1800**	**Var %**
3	23	60 Hz	65	625	406	323	255	166	117	89	74	11%
5	28			619	407	325	260	174	126	97	80	13%
7	31			605	402	325	262	178	129	99	82	9%
3	24	150 Hz		577	371	294	231	150	106	79	65	
5	29			552	363	291	231	153	110	84	69	
7	31			567	374	300	240	162	118	89	74	
3	23	60 Hz	90	804	526	417	330	221	162	128	107	13%
5	28			836	554	446	359	247	182	142	118	14%
7	31			844	571	464	375	261	191	149	124	10%
3	23	150 Hz		726	470	373	295	195	142	112	93	
5	27			738	486	391	315	216	159	125	102	
7	30			778	522	422	341	235	172	134	110	

LP – Number of load plates used which directly influence drop height, PT – Pulse time [ms], SF – Smoothing filter setting, Load – Nominal peak load [kN], Var % - Percentage variation of deflection when comparing results with SF set to 150 Hz and 60 Hz

Table. II.2 - Smoothing filter test results, LNEC rigid pavement

		Distance [mm] (Deflection [μm])								
SF	**Load**	**0**	**300**	**450**	**600**	**900**	**1200**	**1500**	**1800**	**Var %**
0	90	98%	98%	98%	98%	97%	97%	97%	99%	98%
60 Hz	90	105%	105%	105%	105%	104%	104%	104%	106%	105%
150 Hz	90	100%	100%	100%	100%	100%	100%	100%	100%	
200 Hz	90	99%	99%	99%	99%	99%	99%	97%	101%	99%

SF – Smoothing filter setting, Load – Nominal peak load [kN], Var % - Percentage variation of deflection when comparing results with SF set to 150 Hz

Appendix III. Repeatability and Reproducibility, N=3

Table. III.1 – Cochran's test

	0	300	450	600	900	1200	1500	1800	Load
65 Flexible	OK	FWD3***	FWD3*	OK	FWD3*	FWD3***	FWD3*	FWD3***	OK
90 Flexible	OK	OK	OK	OK	OK	OK	FWD2*	OK	OK
90 Rigid	FWD2***	FWD2***	OK	OK	OK	FWD2***	OK	OK	OK

OK – Accept, * - Suspect outlier (95%), ** - Reject outlier (99%), *** - Suspect (95%) and Reject outlier (99%)

Table. III.2 - Grubb's test

	0	300	450	600	900	1200	1500	1800	Load
65 Flexible	OK	OK	OK	OK	OK	OK	OK	OK	OK
90 Flexible	OK	OK	OK	OK	OK	OK	OK	OK	OK
90 Rigid	OK	OK	OK	OK	OK	OK	OK	OK	OK

OK – Accept, * - Suspect outlier (95%), ** - Reject outlier (99%), *** - Suspect (95%) and Reject outlier (99%)

Table. III.3 - Site 1, 65 kN

	0	300	450	600	900	1200	1500	1800
X	668.20	499.60	408.60	338.80	237.50	180.60	140.10	124.30
σ	119.99	97.52	77.96	67.37	51.91	42.52	31.26	31.56
σ_r^2	4.22	8.67	7.44	0.67	7.56	22.33	10.11	2.33
σ_d^2	43189.59	28533.17	18231.80	13617.77	8082.50	5425.01	2932.29	2989.01
σ_L^2	14395.12	9508.17	6074.78	4539.03	2691.5	1800.89	974.06	995.56
σ_R^2	14399.34	9516.83	6082.23	4539.70	2699.20	1823.22	984.17	997.89
CV_r	0.3%	0.6%	0.7%	0.2%	1.2%	2.6%	2.3%	1.2%
CV_R	18.0%	19.5%	19.1%	19.9%	21.9%	23.6%	22.4%	25.4%
r	5.82	8.33	7.72	2.31	7.78	13.37	9.00	4.32
R	339.59	276.08	220.71	190.68	147.03	120.84	88.78	89.40

X – mean of means, σ - standard deviation, σ_r^2 – repeatability variance, σ_d^2 - intralaboratory variance, σ_L^2 – interlaboratory variance, σ_R^2 - repeatability variance, CV_r – repeatability coefficient of variation, CV_R – reproducibility variance, r – repeatability, R – reproducibility

Table. III.4 - Site 1, 90 kN

	0	300	450	600	900	1200	1500	1800
X	863.10	655.30	540.50	447.10	314.00	238.70	195.10	167.40
σ	133.40	116.25	92.91	79.24	58.04	46.51	40.14	35.62
σ_r^2	4.56	3.89	4.89	1.78	4.33	2.56	1.78	0.67
σ_d^2	53390.30	40542.08	25897.10	18835.29	10107.00	6489.98	4833.39	3807.17
σ_L^2	17795.25	13512.73	8630.74	6277.84	3367.56	2162.47	1610.54	1268.83
σ_R^2	17799.80	13516.62	8635.62	6279.62	3371.89	2165.03	1612.32	1269.50
CV_r	0.2%	0.3%	0.4%	0.3%	0.7%	0.7%	0.7%	0.5%
CV_R	15.5%	17.7%	17.2%	17.7%	18.5%	19.5%	20.6%	21.3%
R	6.04	5.58	6.26	3.77	5.89	4.52	3.77	2.31
R	377.57	329.02	262.99	224.26	164.33	131.68	113.63	100.83

X – Mean of means, σ - standard deviation, σ_r^2 – repeatability variance, σ_d^2 - intralaboratory variance- σ_L^2 – interlaboratory variance, σ_R^2 - repeatability variance, CV_r – repeatability coefficient of variation, CV_R – reproducibility variance, r – repeatability, R – reproducibility, IC 95% - critical value for IC 95% normal distribution, IC 80% - critical value for IC 80% normal distribution

Table. III.5 - Site 2, 90 kN

	0	300	450	600	900	1200	1500	1800
X	321.80	285.10	262.40	240.70	197.70	162.80	134.40	110.70
σ	34.31	32.23	30.07	27.74	22.27	19.89	16.93	15.08
σ_r^2	0.44	0.11	0.44	0.67	0.22	0.11	0.44	0.22
σ_d^2	3530.60	3117.09	2713.10	2308.01	1488.08	1187.00	860.30	682.28
σ_L^2	1176.72	1038.99	904.22	769.11	495.95	395.63	286.62	227.35
σ_R^2	1177.16	1039.10	904.66	769.78	496.17	395.74	287.06	227.57
CV_r	0.2%	0.1%	0.3%	0.3%	0.2%	0.2%	0.5%	0.4%
CV_R	10.7%	11.3%	11.5%	11.5%	11.3%	12.2%	12.6%	13.6%
r	1.89	0.94	1.89	2.31	1.33	0.94	1.89	1.33
R	97.10	91.23	85.12	78.52	63.04	56.30	47.95	42.69

X – Mean of means, σ - standard deviation, σ_r^2 – repeatability variance, σ_d^2 - intralaboratory variance- σ_L^2 – interlaboratory variance, σ_R^2 - repeatability variance, CV_r – repeatability coefficient of variation, CV_R – reproducibility variance, r – repeatability, R – reproducibility, IC 95% - critical value for IC 95% normal distribution, IC 80% - critical value for IC 80% normal distribution

Appendix IV. Repeatability and Reproducibility, N=2

Table. IV.1 – Cochran's test

	0	300	450	600	900	1200	1500	1800	Load
65 Flexible	OK	FWD3*	OK	OK	OK	FWD3*	OK	FWD3***	OK
90 Flexible	OK	OK	OK	OK	OK	OK	OK	OK	OK
90 Rigid	FWD2***	FWD2***	FWD2***	FWD2***	OK	FWD2***	OK	FWD2***	OK

OK – Accept, * - Suspect outlier (95%), ** - Reject outlier (99%), *** - Suspect (95%) and Reject outlier (99%)

Table. IV.2 - Grubb's test

	0	300	450	600	900	1200	1500	1800	Load
65 Flexible	OK	OK	OK	OK	OK	OK	OK	OK	OK
90 Flexible	OK	OK	OK	OK	OK	OK	OK	OK	OK
90 Rigid	OK	OK	OK	OK	OK	OK	OK	OK	OK

OK – Accept, * - Suspect outlier (95%), ** - Reject outlier (99%), *** - Suspect (95%) and Reject outlier (99%)

Table. IV.3 - Site 1, 65 kN

	0	300	450	600	900	1200	1500	1800
X	735.70	555.50	453.50	377.50	267.30	204.80	158.20	142.50
σ	38.679	15.839	6.364	8.768	8.485	10.607	0.212	3.536
σ_r^2	6.17	12.83	11.00	0.83	11.33	33.33	15.17	3.50
σ_d^2	4488.15	752.64	121.50	230.64	216.00	337.50	0.15	37.50
σ_L^2	747.00	123.30	18.42	38.30	34.11	50.69	-2.50	5.67
σ_R^2	753.16	136.13	29.42	39.13	45.44	84.03	12.66	9.17
CV_r	0.3%	0.6%	0.7%	0.2%	1.3%	2.8%	2.5%	1.3%
CV_R	3.7%	2.1%	1.2%	1.7%	2.5%	4.5%	2.2%	2.1%
r	7.0	10.1	9.4	2.6	9.5	16.3	11.0	5.3
R	77.7	33.0	15.3	17.7	19.1	25.9	10.1	8.6

X – mean of means, σ - standard deviation, σ_r^2 – repeatability variance, σ_d^2 - intralaboratory variance, σ_L^2 – interlaboratory variance, σ_R^2 - repeatability variance, CV_r – repeatability coefficient of variation, CV_R – reproducibility variance, r – repeatability, R – reproducibility

Table. IV.4 - Site 1, 90 kN

	0	300	450	600	900	1200	1500	1800
X	939.90	722.40	594.20	492.70	347.50	265.50	218.20	188.00
σ	16.758	8.980	4.031	10.394	2.121	2.546	5.869	0.424
σ_r^2	1.67	3.67	3.17	0.67	5.00	3.33	2.17	0.83
σ_d^2	842.55	241.95	48.75	324.15	13.50	19.44	103.35	0.54
σ_L^2	140.15	39.71	7.60	53.91	1.42	2.68	16.86	-0.05
σ_R^2	141.81	43.38	10.76	54.58	6.42	6.02	19.03	0.78
CV_r	0.1%	0.3%	0.3%	0.2%	0.6%	0.7%	0.7%	0.5%
CV_R	1.3%	0.9%	0.6%	1.5%	0.7%	0.9%	2.0%	0.5%
R	3.7	5.4	5.0	2.3	6.3	5.2	4.2	2.6
R	33.7	18.6	9.3	20.9	7.2	6.9	12.3	2.5

X – Mean of means, σ - standard deviation, σ_r^2 – repeatability variance, σ_d^2 - intralaboratory variance- σ_L^2 – interlaboratory variance, σ_R^2 - repeatability variance, CV_r – repeatability coefficient of variation, CV_R – reproducibility variance, r – repeatability, R – reproducibility, IC 95% - critical value for IC 95% normal distribution, IC 80% - critical value for IC 80% normal distribution

Table. IV.5 - Site 2, 90 kN

	0	300	450	600	900	1200	1500	1800
X	340.70	303.20	279.00	256.00	210.00	173.70	143.70	118.90
σ	14.637	11.102	12.728	11.314	8.910	8.980	7.990	7.283
σ_r^2	0.67	0.17	0.50	0.50	0.33	0.17	0.67	0.17
σ_d^2	642.75	369.75	486.00	384.00	238.14	241.95	191.55	159.15
σ_L^2	107.01	61.60	80.92	63.92	39.63	40.30	31.81	26.50
σ_R^2	107.68	61.76	81.42	64.42	39.97	40.46	32.48	26.66
CV_r	0.2%	0.1%	0.3%	0.3%	0.3%	0.2%	0.6%	0.3%
CV_R	3.0%	2.6%	3.2%	3.1%	3.0%	3.7%	4.0%	4.3%
r	2.3	1.2	2.0	2.0	1.6	1.2	2.3	1.2
R	29.4	22.2	25.5	22.7	17.9	18.0	16.1	14.6

X – Mean of means, σ - standard deviation, σ_r^2 – repeatability variance, σ_d^2 - intralaboratory variance- σ_L^2 – interlaboratory variance, σ_R^2 - repeatability variance, CV_r – repeatability coefficient of variation, CV_R – reproducibility variance, r – repeatability, R – reproducibility, IC 95% - critical value for IC 95% normal distribution, IC 80% - critical value for IC 80% normal distribution

Appendix V. Critical values

Table. V.1 – Critical values, Site 1, 65 kN

		0	300	450	600	900	1200	1500	1800
N=3	X	668	499	409	339	238	181	140	124
	σ	119.99	97.52	77.96	67.37	51.91	42.52	31.26	31.56
	CRV	235	191	153	132	102	83	61	62
N=2	X	736	556	454	378	267	205	158	143
	σ	38.68	15.84	6.36	8.77	8.49	10.61	0.21	3.54
	CRV	76	31	21	17	17	21	0	7

X – Mean of means, σ - standard deviation, CRV - critical value for IC 95% normal distribution

Table. V.2 – Critical values. Site 1, 90 kN

		0	300	450	600	900	1200	1500	1800
N=3	X	863	655	541	447	314	239	195	167
	σ	133.40	116.25	92.91	79.24	58.04	46.51	40.14	35.62
	CRV	261	228	182	155	114	91	79	70
N=2	X	940	722	594	493	348	266	218	188
	σ	16.76	8.98	4.03	10.39	2.12	2.55	5.87	0.42
	CRV	33	18	8	20	4	5	12	1

X – Mean of means, σ - standard deviation, CRV - critical value for IC 95% normal distribution

Table. V.3 – Critical values, Site 2, 90 kN

		0	300	450	600	900	1200	1500	1800
N=3	X	322	285	262	241	198	163	134	111
	σ	34.31	32.23	30.07	27.74	22.27	19.89	16.93	15.08
	CRV	67	63	59	54	44	39	33	30
N=2	X	341	303	279	256	210	174	144	119
	σ	14.64	11.10	12.73	11.31	8.91	8.98	7.99	7.28
	CRV	29	22	25	22	17	18	16	14

X – Mean of means, σ - standard deviation, CRV - critical value for IC 95% normal distribution

Appendix VI. Pavement structures

Table. VI.1 – Reference layer moduli

Pavement type	Pavement model	Reference moduli	
F3, asphalt bound base		**AC**	4000
		UGM	200
		Subgrade	100
		RL	1000
F3, asphalt bound base		**AC**	4000
		UGM	200
		Subgrade	100
		RL	1000
F3, unbound aggregate base		**AC**	4000
		UGM	400
		UGM	200
		Subgrade	100
		RL	1000
F3, unbound aggregate base	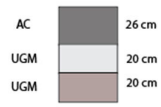	**AC**	4000
		UGM	400
		UGM	200
		Subgrade	100
		RL	1000
F2, asphalt bound base		**AC**	4000
		UGM	120
		Subgrade	60
		RL	1000
F2, asphalt bound base	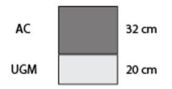	**AC**	4000
		UGM	120
		Subgrade	60
		RL	1000
F2, unbound aggregate base		**AC**	4000
		UGM	240
		UGM	120
		Subgrade	60
		RL	1000

Pavement type	Pavement model	Reference moduli
F2, unbound aggregate base	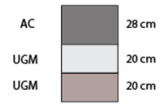	**AC** 4000 **UGM** 240 **UGM** 120 **Subgrade** 60 **RL** 1000

AC -asphalt concrete, UGM – unbound granular material, RL – rigid layer, Measuring unit - MPa

Appendix VII. Backcalculation of pavement structures

Table. VII.1 - F3, asphalt bound base 0.12, 65 kN

	Deflection	D_{low}	D_{high}	BC_{low}	E_{max}	BC_{high}	E_{min}
0	593	390	796	391	4700	809	3000
300	360	224	496	217	300	500	160
450	249	148	350	142	175	352	70
600	170	96	244	92	3000	244	600
900	77	38	116	38	4700	116	
1200	34	14	55	15		55	
1500	16	5	26	5		26	
1800	8	2	14	2		14	
			RMS%	3.6		0.9	

Table. VII.2 - F3, asphalt bound base 0.28, 65 kN

	Deflection	D_{low}	D_{high}	BC_{low}	E_{max}	BC_{high}	E_{min}
0	273	164	382	176	4500	382	3000
300	198	114	282	115	400	281	140
450	166	93	238	92	200	237	70
600	137	75	199	73	2500	197	600
900	89	45	133	43		130	
1200	55	25	85	24		82	
1500	33	13	52	13		50	
1800	19	6	31	6,		30	
			RMS%	3.6		2.3	

Table. VII.3 - F3, unbound granular base 0.10, 65 kN

	Deflection	D_{low}	D_{high}	BC_{low}	E_{max}	BC_{high}	E_{min}
0	513	332	694	335	4300	691	3300
300	296	180	412	173	600	412	300
450	211	123	300	118	330	299	150
600	154	86	223	83	180	221	70
900	84	42	126	42	3500	124	600
1200	46	20	72	21		70	
1500	25	9	41	10		40	
1800	14	4	23	4		23	
			RMS%	2.8		1.5	

Table. VII.4 - F3, unbound granular base 0.26

	Deflection	D_{low}	D_{high}	BC_{low}	E_{max}	BC_{high}	E_{min}
0	260	156	365	157	5000	354	3300
300	186	106	265	103	750	260	290
450	156	87	224	83	360	220	130
600	129	70	188	67	200	185	70
900	87	44	129	42	3000	127	600
1200	56	26	87	25		84	
1500	36	15	57	15		55	
1800	22	8	36	8		35	
			RMS%	3.6		2.5	

Units: Deflection μm, Elastic modulus: MPa; Deflection – simulated deflection measurement, D_{low} – lower critical interval for deflections, D_{high} – upper critical interval for deflections, BC_{low} – backcalculated deflection for lower CI, BC_{high} – backcalculated deflection for upper CI, E_{max} – estimated moduli for lower CI, E_{min} – estimated moduli for upper CI

Table. VII.5 - F2, asphalt bound base 0.16, 65 kN

	Deflection	D_{low}	D_{high}	BC_{low}	E_{max}	BC_{high}	E_{min}
0	629	416	842	421	4800	846	3000
300	449	287	612	285	200	607	90
450	348	216	480	214	100	471	45
600	262	157	367	156	2700	356	580
900	138	75	201	76		191	
1200	66	32	101	33		94	
1500	28	11	46	12		43	
1800	10	3	18	3		18	
			RMS%	3.9		3.9	

Table. VII.6 - F2, asphalt bound base 0.32, 65 kN

	Deflection	D_{low}	D_{high}	BC_{low}	E_{max}	BC_{high}	E_{min}
0	303	185	421	198	5000	408	3200
300	232	137	328	144	200	319	90
450	203	118	288	122	110	281	40
600	175	99	251	103	3000	245	750
900	125	67	183	69		178	
1200	85	43	127	44		123	
1500	55	25	85	26		82	
1800	34	14	54	14		51	
			RMS%	3.9		3.2	

Table. VII.7 - F2, unbound granular base 0.12, 65 kN

	Deflection	D_{low}	D_{high}	BC_{low}	E_{max}	BC_{high}	E_{min}
0	665	442	888	437	4500	867	3500
300	439	279	598	267	380	586	175
450	328	202	454	192	190	444	90
600	244	145	344	139	105	334	45
900	135	73	196	72	3500	188	550
1200	72	35	109	36		104	
1500	37	15	59	16		56	
1800	18	6	30	6		29	
			RMS%	3.3		3.2	

Table. VII.8 - F2, unbound granular base 0.28, 65 kN

	Deflection	D_{low}	D_{high}	BC_{low}	E_{max}	BC_{high}	E_{min}
0	322	198	446	201	5000	440	3000
300	246	146	346	144	440	339	190
450	213	124	301	121	220	295	90
600	182	104	260	101	115	253	45
900	128	69	187	68	2500	182	450
1200	87	44	130	44		127	
1500	56	26	87	27		86	
1800	35	14	56	15		56	
			RMS%	2.8		2.0	

Units: Deflection μm, Elastic modulus: MPa; Deflection – simulated deflection measurement, D_{low} – lower critical interval for deflections, D_{high} – upper critical interval for deflections, BC_{low} – backcalculated deflection for lower CI, BC_{high} – backcalculated deflection for upper CI, E_{max} – estimated moduli for lower CI, E_{min} – estimated moduli for upper CI

Table. VII.9 - F3, asphalt bound base 0.12, 90 kN

	Deflection	D_{low}	D_{high}	BC_{low}	E_{max}	BC_{high}	E_{min}
0	821	557	1086	558	4500	1120	3000
300	499	322	675	312	310	692	180
450	345	214	476	206	165	487	70
600	235	139	331	134	2750	338	800
900	107	56	157	56		160	
1200	48	21	74	22		76	
1500	22	8	36	8		37	
1800	11	3	19	3		20	
			RMS%	4.0		2.7	

Table. VII.10 - F3, asphalt bound base 0.28, 90 kN

	Deflection	D_{low}	D_{high}	BC_{low}	E_{max}	BC_{high}	E_{min}
0	378	237	519	238	5000	529	3500
300	274	165	383	160	390	388	150
450	229	135	324	129	190	328	75
600	189	108	270	103	2400	272	700
900	123	66	180	63		180	
1200	76	37	115	36		114	
1500	45	20	70	20		69	
1800	26	10	42	10		41	
			RMS%	3.5		1.2	

Table. VII.11 - F3, unbound granular base 0.10, 90 kN

	Deflection	D_{low}	D_{high}	BC_{low}	E_{max}	BC_{high}	E_{min}
0	710	475	945	484	4300	957	3300
300	410	259	561	258	600	571	300
450	293	178	407	178	310	414	150
600	213	124	302	126	160	306	70
900	117	62	172	65	3500	172	600
1200	64	30	98	32		97	
1500	35	14	55	15		55	
1800	19	6	31	6		32	
			RMS%	3.9		1.0	

Table. VII.12 - F3, unbound granular base 0.26, 90 kN

	Deflection	D_{low}	D_{high}	BC_{low}	E_{max}	BC_{high}	E_{min}
0	361	225	497	225	5000	489	3300
300	257	154	361	148	700	360	290
450	215	126	305	120	360	305	130
600	179	102	256	97	190	256	70
900	120	64	176	62	2500	176	700
1200	78	38	117	38		117	
1500	49	22	77	23		76	
1800	31	12	49	13		49	
			RMS%	3.9		0.7	

Units: Deflection μm, Elastic modulus: MPa; Deflection – simulated deflection measurement, D_{low} – lower critical interval for deflections, D_{high} – upper critical interval for deflections, BC_{low} – backcalculated deflection for lower CI, BC_{high} – backcalculated deflection for upper CI, E_{max} – estimated moduli for lower CI, E_{min} – estimated moduli for upper CI

Table. VII.13– F2, asphalt bound base 0.16, 90 kN

	Deflection	D_{low}	D_{high}	BC_{low}	E_{max}	BC_{high}	E_{min}
0	871	594	1148	584	4800	1172	3000
300	622	411	833	396	200	840	110
450	481	310	653	297	100	652	45
600	362	226	499	216	2500	493	800
900	191	110	273	106		264	
1200	92	47	137	47		131	
1500	39	17	62	17		60	
1800	14	4	24	4		25	
			RMS%	3.5		2.9	

Table. VII.14 – F2, asphalt bound base 0.32, 90 kN

	Deflection	D_{low}	D_{high}	BC_{low}	E_{max}	BC_{high}	E_{min}
0	419	265	572	274	5000	565	3000
300	322	198	446	199	180	442	100
450	281	170	392	170	90	390	50
600	242	144	341	142	2000	339	500
900	173	98	248	96		246	
1200	118	63	173	60		171	
1500	76	37	115	36		113	
1800	47	21	73	19		71	
			RMS%	3.6		1.7	

Table. VII.15 – F2, unbound granular base 0.12, 90 kN

	Deflection	D_{low}	D_{high}	BC_{low}	E_{max}	BC_{high}	E_{min}
0	921	631	1211	627	4500	1200	3500
300	607	400	814	386	360	812	175
450	454	290	618	279	185	615	90
600	338	209	467	202	100	463	45
900	187	107	266	105	3000	261	550
1200	100	52	148	52		144	
1500	51	23	79	24		78	
1800	25	9	40	9		41	
			RMS%	2.9		1.7	

Table. VII.16 – F2, unbound granular base 0.28, 90 kN

	Deflection	D_{low}	D_{high}	BC_{low}	E_{max}	BC_{high}	E_{min}
0	446	285	608	289	5000	591	3500
300	341	211	471	209	400	466	170
450	295	179	410	176	200	408	85
600	252	150	353	147	110	354	40
900	178	101	254	99	2500	257	650
1200	120	64	176	63		179	
1500	78	39	118	38		120	
1800	49	22	75	22		77	
			RMS%	1.6		1.8	

Units: Deflection μm, Elastic modulus: MPa; Deflection – simulated deflection measurement, D_{low} – lower critical interval for deflections, D_{high} – upper critical interval for deflections, BC_{low} – backcalculated deflection for lower CI, BC_{high} – backcalculated deflection for upper CI, E_{max} – estimated moduli for lower CI, E_{min} – estimated moduli for upper CI

Table. VII.17 - Sensitivity analysis, Percentage of top layer over pavement total thickness

	F3, 65 kN		
Asphalt bound base	0.12m	Top	Bottom
	4000	18%	-25%
	200	50%	-20%
	100	75%	-30%
	0.28m	Top	Bottom
	4000	13%	-25%
	200	100%	-30%
	100	100%	-30%
		13%	-25%
Unbound granular base	0.10m	Top	Bottom
	4000	8%	-18%
	400	50%	-25%
	200	65%	-25%
	100	80%	-30%
	0.26m	Top	Bottom
	4000	25%	-18%
	400	88%	-28%
	200	80%	-35%
	100	100%	-30%

F3, 90 kN		
0.12m	Top	Bottom
4000	13%	-25%
200	55%	-10%
100	65%	-30%
0.28m	Top	Bottom
4000	25%	-13%
200	95%	-25%
100	90%	-25%
0.10m	Top	Bottom
4000	8%	-18%
400	50%	-25%
200	55%	-25%
100	60%	-30%
0.26m	Top	Bottom
4000	25%	-18%
400	75%	-28%
200	80%	-35%
100	90%	-30%

F2, 65 kN		
0.16m	Top	Bottom
4000	20%	-25%
120	67%	-25%
60	67%	-25%
0.32m	Top	Bottom
4000	25%	-20%
120	67%	-25%
60	83%	-33%
0.12m	Top	Bottom
4000	13%	-13%
240	58%	-27%
120	58%	-25%
60	75%	-25%
0.28m	Top	Bottom
4000	25%	-25%
240	83%	-21%
120	83%	-25%
60	92%	-25%

F2, 90 kN		
0.16m	Top	Bottom
4000	20%	-25%
120	67%	-8%
60	67%	-25%
0.32m	Top	Bottom
4000	25%	-25%
120	50%	-17%
60	50%	-17%
0.12m	Top	Bottom
4000	13%	-13%
240	50%	-27%
120	54%	-25%
60	67%	-25%
0.28m	Top	Bottom
4000	25%	-13%
240	67%	-29%
120	67%	-29%
60	83%	-33%

Units: Elastic modulus: MPa; Top – upper threshold (softer layer), Bottom – lower threshold – (stiffer layer)

Appendix VIII. Test site 1 backcalculation

Table. VIII.1 – Test site 1 backcalculation

FWD 1, 65 kN

	Deflection	BC	E	Thickness
0	534	593	6500	0.050
300	388	364	650	0.200
450	319	299	700	0.150
600	262	252	110	0.150
900	178	181	60	1.000
1200	133	131	200	
1500	104	95		
1800	88	70		
	RMS%	9.3		

FWD 1, 90 kN

	Deflection	BC	E	Thickness
0	712	737	7000	0.050
300	523	475	850	0.200
450	435	398	700	0.150
600	358	340	150	0.150
900	248	250	60	1.000
1200	185	184		
1500	149	136		
1800	126	102		
	RMS%	8.8		

FWD 2, 65 kN

	Deflection	BC	E	Thickness
0	708	746	6000	0.050
300	544	492	600	0.200
450	449	418	600	0.150
600	371	363	90	0.150
900	261	277	50	1.000
1200	197	215		
1500	158	168		
1800	140	134		
	RMS%	6.5		

FWD 2, 90 kN

	Deflection	BC	E	Thickness
0	928	992	6000	0.050
300	716	643	600	0.200
450	591	542	600	0.150
600	485	469	90	0.150
900	346	358	60	1.000
1200	264	277		
1500	214	219		
1800	188	176		
	RMS%	6.2		

FWD 3, 65 kN

	Deflection	BC	E	Thickness
0	763	813	7000	0.050
300	566	534	500	0.200
450	458	449	600	0.150
600	384	388	75	0.150
900	273	293	40	1.000
1200	212	223		
1500	158	171		
1800	145	133		
	RMS%	6.1		

FWD 3, 90 kN

	Deflection	BC	E	Thickness
0	952	991	6500	0.050
300	729	661	650	0.200
450	597	560	600	0.150
600	500	485	80	0.150
900	349	368	50	1.000
1200	267	282		
1500	222	218		
1800	188	172		
	RMS%	6.0		

Units: Deflection μm, Elastic modulus: MPa, Layer thickness: m; Deflection – measured "in-situ" deflection, BC – backcalculated deflection, E – estimated moduli, thickness – Layer thickness

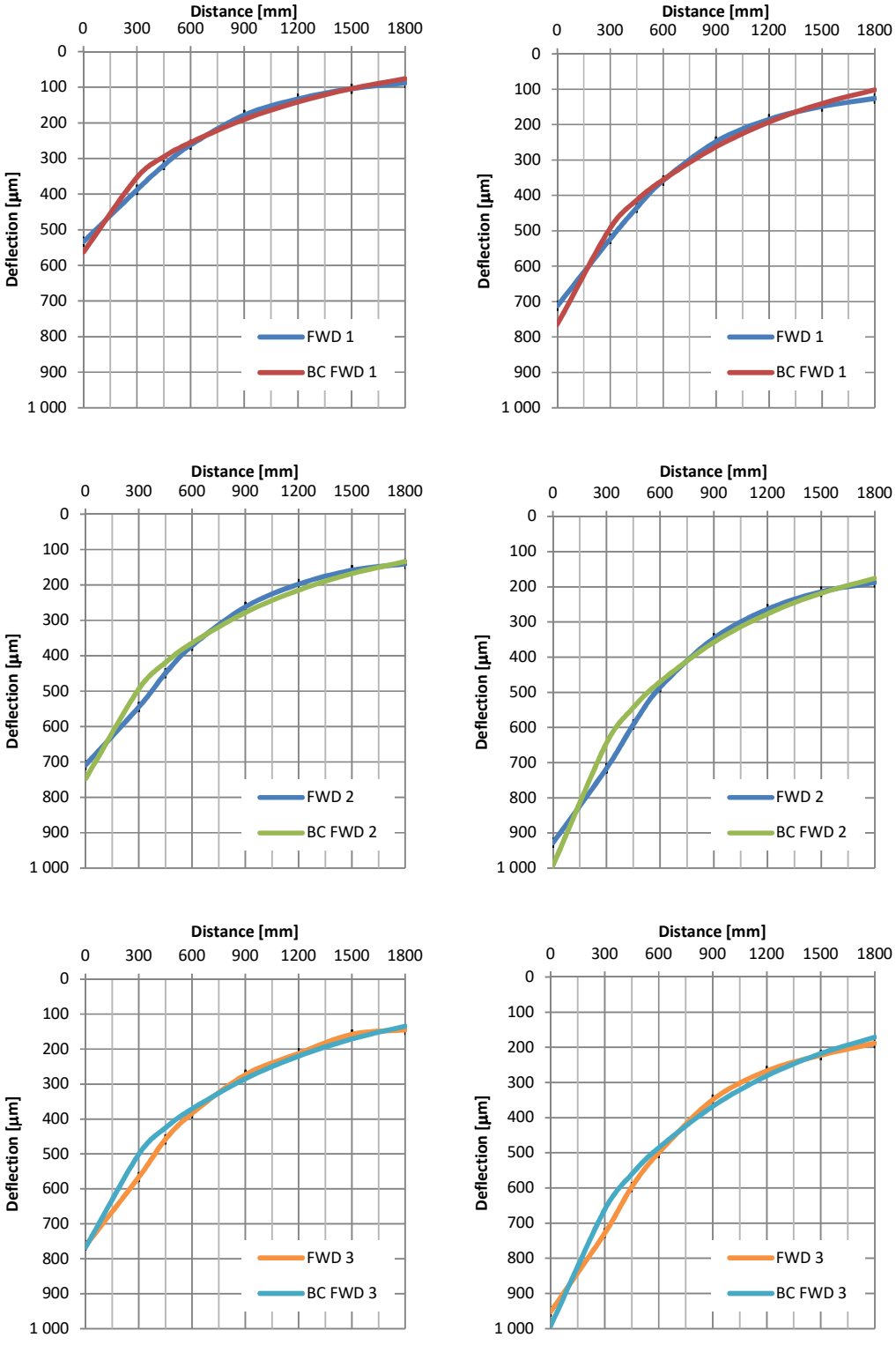

Figure. VIII.1 - Backcalculated deflections (65 kN and 90 kN)